

Spatial Organization of Receptive Fields of V1 Neurons of Alert Monkeys: Comparison With Responses to Gratings

IGOR KAGAN,¹ MOSHE GUR,^{1,2} AND D. MAX SNODDERLY^{2–4}

¹Department of Biomedical Engineering, Technion, Israel Institute of Technology, Haifa 32000, Israel; ²Schepens Eye Research Institute, Boston, Massachusetts 02114; and ³Department of Ophthalmology, and ⁴Program in Neuroscience, Harvard Medical School, Boston, Massachusetts 02115

Received 18 October 2001; accepted in final form 2 August 2002

Kagan, Igor, Moshe Gur, and D. Max Snodderly. Spatial organization of receptive fields of V1 neurons of alert monkeys: comparison with responses to gratings. *J Neurophysiol* 88: 2557–2574, 2002; 10.1152/jn.00858.2001. We studied the spatial organization of receptive fields and the responses to gratings of neurons in parafoveal V1 of alert monkeys. Activating regions (ARs) of 228 cells were mapped with increment and decrement bars while compensating for fixational eye movements. For cells with two or more ARs, the overlap between ARs responsive to increments (INC) and ARs responsive to decrements (DEC) was characterized by a quantitative overlap index (OI). The distribution of overlap indices was bimodal. The larger group (78% of cells) was composed of complex cells with strongly overlapping ARs (OI \geq 0.5). The smaller group (14%) was composed of simple cells with minimal spatial overlap of ARs (OI \leq 0.3). Simple cells were preferentially located in layers dominated by the magnocellular pathway. A third group of neurons, the monocontrast cells (8%), responded only to one sign of contrast and had more sustained responses to flashed stimuli than other cells. One hundred fourteen neurons were also studied with drifting sinusoidal gratings of various spatial frequencies and window widths. For complex cells, the relative modulation (RM, the ratio of the 1st harmonic to the mean firing rate), ranged from 0.6 ± 0.4 to 1.1 ± 0.5 (mean \pm SD), depending on the stimulus conditions and the mode of correction for eye movements. RM was not correlated with the degree of overlap of ARs, indicating that the spatial organization of receptive fields cannot reliably be predicted from RM values. In fact, a subset of complex cells had RM > 1 , the traditional criterion for identifying simple cells. However, unlike simple cells, even those complex cells with high RM could exhibit diverse nonlinear responses when the spatial frequency or window size was changed. Furthermore, the responses of complex cells to counterphase gratings were predominantly nonlinear even harmonics. These results show that RM is not a robust test of linearity. Our results indicate that complex cells are the most frequently encountered neurons in primate V1, and their behavior needs to receive more emphasis in models of visual function.

INTRODUCTION

Hubel and Wiesel (1962, 1968) divided cells in the primary visual cortex of cats and monkeys into two groups—simple and complex. They were distinguished by the spatial organization of the receptive fields; simple cells had small receptive fields with two or three separate ON or OFF zones, whereas complex cells had larger receptive fields with less discrete zones or nonlinear summation properties. More recent work has at-

tempted to match the original dichotomy by characterizing these two types according to their responses to sinusoidal stimuli. A presumed index of linearity, the *relative modulation* (RM, the ratio of the response amplitude at the temporal frequency of a drifting grating to the mean firing rate) was proposed to be >1 for simple cells and <1 for complex cells (De Valois et al. 1982; Movshon et al. 1978; Skottun et al. 1991). However, modulated responses of complex cells have been reported by many authors (Dean and Tolhurst 1983; Foster et al. 1985; Glezer et al. 1980, 1982; Hammond et al. 1989; Holub and Morton-Gibson 1981; Kulikowski and Bishop 1982; Pollen and Ronner 1982; Pollen et al. 1978). Although the majority view equates cell classification by spatial mapping and by relative modulation criteria (Skottun et al. 1991), there are exceptions to this opinion based on studies in cat V1 (Dean and Tolhurst 1983; Hammond et al. 1989).

A stronger inconsistency is present in the literature on monkey visual cortex, where results based on spatial mapping have designated a small minority of V1 neurons (7–22%) as simple cells (Dow 1974; Foster et al. 1985; Gur et al. 1999b; Hubel and Wiesel 1968; Schiller et al. 1976; Snodderly et al. 2000; see also Conway 2001), but with one exception (Prince et al. 2000), use of the relative modulation criterion has resulted in roughly half of monkey V1 neurons (40–60%) being designated as simple cells (De Valois et al. 1982; O’Keefe et al. 1998; Sceniak et al. 1999, 2001). This conflict has not been resolved because no paper on monkey V1 has presented data comparing spatial mapping and relative modulation on the same sample of cells.

The dominance of simple cells in cat V1 and their linear properties have influenced much of the theorizing on functional processing in primary visual cortex (e.g., Artun et al. 1998; Carandini and Heeger 1994; Carandini et al. 1997; Chance et al. 1998; Heeger 1993; Heeger et al. 1996; Reich et al. 2001; Troyer et al. 1998; Wielaard et al. 2001). Numerous studies have confirmed that simple cells can be considered as basically linear (half-wave-rectified) spatiotemporal operators (Carandini et al. 1999). Responses of such operators are relatively easy to predict, analyze, and model. However, if simple cells are a minor fraction of primate V1 neurons, as spatial mapping studies indicate, then models of cortical function relevant to

Address for reprint requests: D. M. Snodderly, Schepens Eye Research Institute, 20 Staniford St., Boston, MA 02114 (E-mail: maxs@vision.eri.harvard.edu).

The costs of publication of this article were defrayed in part by the payment of page charges. The article must therefore be hereby marked “advertisement” in accordance with 18 U.S.C. Section 1734 solely to indicate this fact.

human perception should incorporate more emphasis on other cell types.

These considerations led us to study the simple/complex dichotomy in V1 of alert monkeys. We found that spatial mapping divided most of our V1 sample into two groups. Simple cells (14%) had nonoverlapping increment (INC)- and decrement (DEC)-responsive zones, whereas complex cells (78%) had overlapping zones. The RM classification was not equivalent to the overlap/nonoverlap dichotomy. Thus for monkey V1, the relatively large number of simple cells found by modulation criteria appears to result from cells with extensively overlapping INC and DEC zones being designated as simple cells. Furthermore, complex cells with high RM values still exhibit essential nonlinearities. The dominance of nonlinear cells with overlapping INC and DEC regions implies that they should be important components in realistic models of visual cortex function.

Parts of this work have been presented in abstract form (Gur et al. 1999b; Snodderly et al. 2000).

METHODS

Five adult female monkeys (2 *Macaca fascicularis* and 3 *M. mulatta*) were used as subjects for spatial mapping, and three of the monkeys—two *M. mulatta* and one *M. fascicularis*—were used for the grating experiments. Monkeys were trained to fixate on a light-emitting diode (LED) for water reward. Once the monkey learned the task, a head-holding implant and a recording well were surgically attached to the skull under deep anesthesia. All procedures complied with National Institutes of Health guidelines and were approved by the Animal Care and Use Committee of the Schepens Eye Research Institute.

Nerve-spike and eye-movement recording

Fiber electrodes made from quartz-insulated platinum-tungsten alloy (Eckhorn and Thomas 1993) with bare tip lengths of $\leq 5 \mu\text{m}$ and impedance at 1 kHz of 3–4 M Ω were most frequently used to record single-unit activity. In some experiments, glass-insulated platinum-iridium electrodes (Snodderly 1973) with a tip diameter of 1–1.5 μm , and bare tip length of 5–7 μm , were used. Cells were assigned to cortical layers based on histological and/or physiological criteria as previously described (Snodderly and Gur 1995).

Position of the dominant eye was monitored by a double Purkinje image eye tracker (2- to 3-minarc resolution; 100-Hz sampling rate) and recorded in a computer file, together with spike arrival times (0.1-ms time resolution) and spike shapes collected at 10–20 kHz (Gur et al. 1999a). The trial started when the monkey correctly pressed the lever in response to the LED and continued for 5 s provided that the gaze remained within a predefined fixation window, usually about $\pm 1.5^\circ$.

Stimulus presentation

Bar and grating stimuli were displayed on a Barco 7351 monitor at a 60-Hz noninterlaced frame rate, with a Truevision ATVista video graphics adapter. Bars were optimized for orientation, length, velocity, and color (green or red), 0.9 log units brighter or darker than the background of 1 cd/m^2 . This luminance is in the low photopic range and stimuli are vividly colored. Chromatic stimuli were generated by activation of individual guns of the monitor. Incremental (bright) bars were presented on a neutral gray background; decremental (dark) bars were presented on a background of a single color (Snodderly and Gur 1995). Because of limitations in the experimental setup, dark bars with the same luminance decrement for both colors could only be

generated from colored backgrounds. Preliminary tests with our new system showed no noticeable difference between ARs mapped with luminance increments and decrements presented on a color or a gray background.

Monochrome sine gratings of 50% luminance contrast, optimal orientation, length, and color were presented on backgrounds of the same color as the decrement bars, with a mean luminance of 1 or 5 cd/m^2 . Gratings had the same mean luminance as the background or were presented so that the maximal luminance corresponded to the luminance of the increment bar. We did not find any difference in responses to these similar luminance conditions.

After the ocular dominance was established, stimuli were viewed binocularly, unless responses during monocular viewing were substantially stronger. The eye position signal for the dominant eye was added to the stimulus position signal at the beginning of each video frame (bars) or each second frame (gratings; “image stabilization,” Gur and Snodderly 1987, 1997a,b; Snodderly and Gur 1995). This was done to compensate for changes in eye position during the intersaccadic intervals. Note that the maximum delay between shifts in the eye position and subsequent corrections could be as long as 28 ms for bars and 44 ms for gratings; thus this procedure was not intended to compensate for the fast saccadic eye movements. Epochs affected by saccades were automatically detected and excluded during data analysis using a velocity threshold of 10°/s (Snodderly et al. 2001) as described in RESULTS.

Receptive field mapping

The width and location of receptive-field activating regions (AR) was estimated with increment and decrement bars (2–16 minarc, mean: 7 ± 3 minarc) swept forward and back at 1.5–7°/s across the receptive field in a direction orthogonal to the optimal orientation axis (Foster et al. 1985; Pettigrew et al. 1968; Schiller et al. 1976). The operational term “activating region” is used to distinguish regions that respond to direct stimulation from other (covert) zones that may modify the directly evoked response (e.g., side inhibition or facilitation from subthreshold regions). To increase the precision of measurement and minimize possible effects of response latency, we calculated AR widths using the lowest velocity that elicited a strong response in the data set for each cell.

Using image stabilization and appropriate eye movement corrections, we were able to obtain reliable measures of AR widths and locations in spite of inevitable variations in fixation (see RESULTS). Average peristimulus time histograms (PSTH) of responses were constructed, and a cumulative curve was superimposed (Fig. 1). The AR width was measured as 95% of the region defined by intersections of least-squares lines fitted to the cumulative curve for the response to motion in the preferred direction. Because our coordinates are referenced to the stimulus center, a quarter width of the bar was subtracted from each side to correct for occasional spikes elicited by incomplete entry and exit of the stimulus (we found that at least a quarter width of an optimal test bar was required to elicit a consistent response).

An overlap index (OI) was calculated as (Schiller et al. 1976)

$$\text{OI} = \frac{0.5 \cdot (\text{INC}_w + \text{DEC}_w) - \text{sep}}{0.5 \cdot (\text{INC}_w + \text{DEC}_w) + \text{sep}} \quad \text{sep} = |\text{INC}_{\text{center}} - \text{DEC}_{\text{center}}| \quad (1)$$

where INC_w and DEC_w denote INC and DEC AR width and sep denotes the separation between INC and DEC centers (defined as centers of mass from cumulative curves for motion in the preferred direction). The OI ranges from negative values for spatially separated INC and DEC ARs to 1 for complete and *symmetric* overlap (illustrated in RESULTS). For simple cells with three ARs ($n = 9$), the mean of two OIs was taken as the measure of overlap. Except for the special case when one AR is completely inside the other, OI is the ratio of the zone of overlap to the total receptive field width. We tested several variations on this formula, but did not find any advantages that would justify modifying it.

A directionality index (DI) was computed as 1 minus the ratio of the response in the nonpreferred direction to the response in the preferred direction, where the response is defined by the cumulative spike count in the same manner as determining the AR. Like other

authors, we classified cells as direction selective when their DI was >0.5 (Snodderly and Gur 1995 and references therein). Except for control experiments, the reported values of OI were always estimated using the preferred direction.

Response latency and a transiency index (TI) (Snodderly et al. 2001) were also assessed for a subset of cells ($n = 101$) stimulated with increment and decrement stationary flashing bars.

Grating responses

Sinusoidal gratings were restricted in space by a rectangular window of optimal length (same length as mapping bars), oriented parallel to the grating bars and centered on the CRF. The width of the window in the direction perpendicular to the orientation axis varied from a fraction of the CRF to a size much wider than the CRF (mean window width: 56 ± 38 minarc; mean window to CRF ratio: 1.9 ± 2.3). Spatial frequency varied from 0.1 to 18 cycles/° (cpd), most frequently from 0.5 to 5 cpd. Two types of gratings—drifting and counterphase (contrast-reversal)—were used. Drifting gratings were usually presented at a temporal frequency of 5 Hz. For directional cells, drift was always in the preferred direction. Counterphase gratings were temporally modulated by a 2-Hz square wave, and in most cells more than one spatial phase was tested.

The fast Fourier transform (FFT) was used to compute the discrete Fourier transform (DFT) of neuronal responses, using as input either the raw concatenated spike train (sequence of 1 and 0 s, where each 1 represents a spike in a spike train sampled at 1 kHz) or a cumulative histogram of spike arrival times averaged over one stimulus cycle. The two methods yielded very similar results for the frequency range of interest. The magnitude (spikes/s) of the response harmonics was extracted as $F_k = (2/N)|\text{DFT}_k|$, $k = 1 \dots N$, where N is the length of the DFT vector. The relative modulation (RM) of the response to a drifting grating [the ratio of the 1st harmonic (F1) to the mean firing rate (F0) with baseline firing rate subtracted] was calculated as (De Valois et al. 1982)

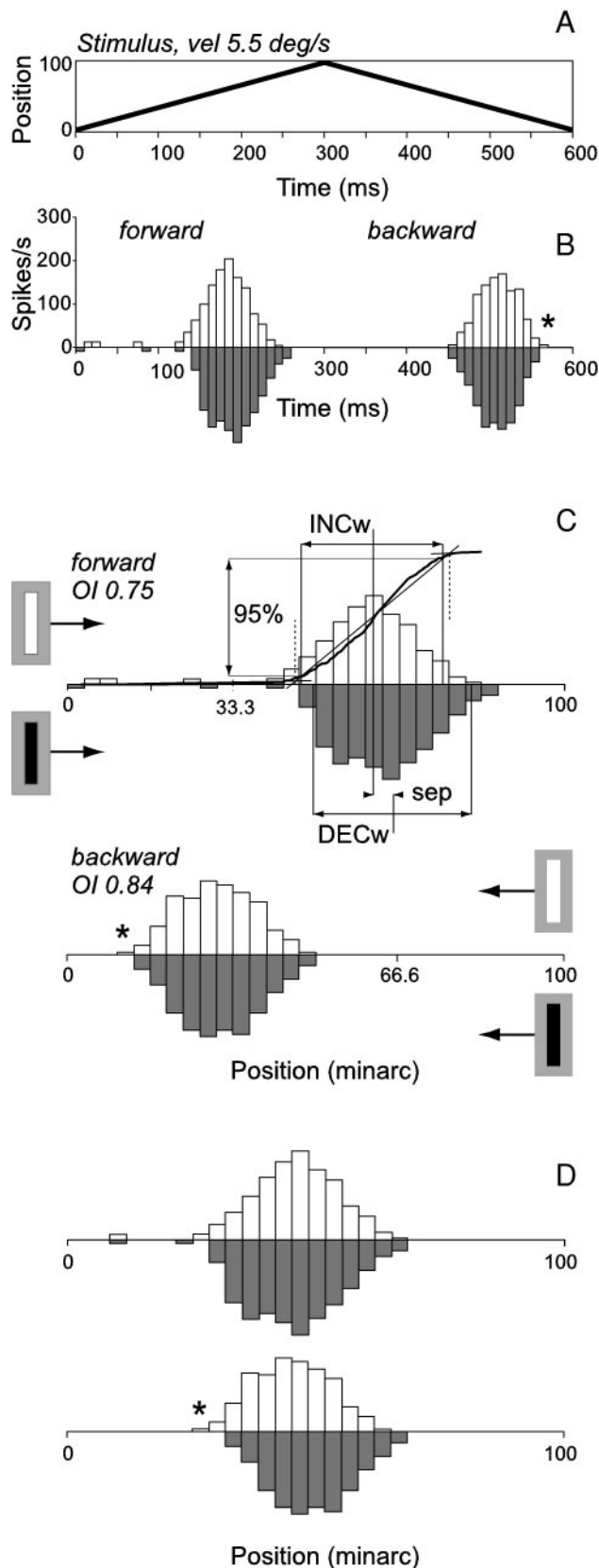
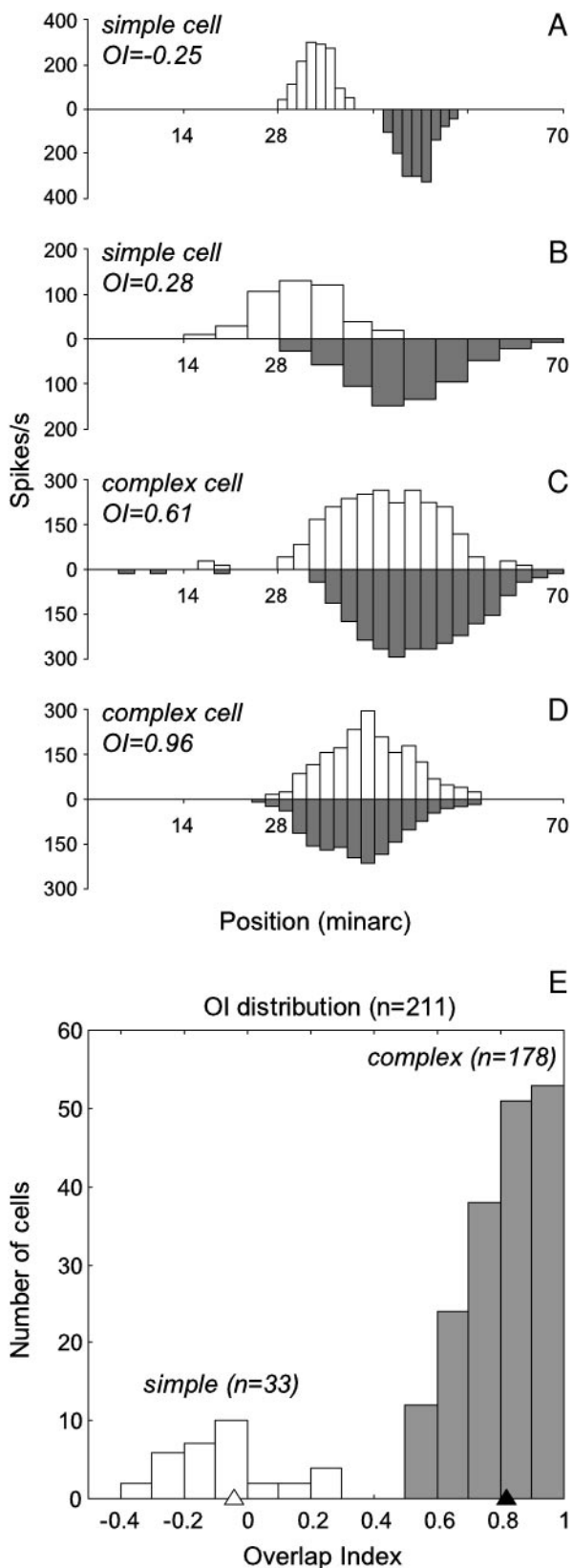


FIG. 1. Spatial mapping of receptive fields. Estimation of width, location and spatial overlap of increment (INC) and decrement (DEC) activating regions (ARs) with sweeping bars. *Complex cell 18602*, INC width (INCw) 26 minarc; DEC width (DECw), 28 minarc; classical receptive field (CRF), 31 minarc; mapping bar, 4 minarc wide. *A*: position of the bar vs. time as it is swept forward across the CRF and back at 5.5°/s. *B*: peristimulus time histograms (PSTHs) of the responses in 2 directions of motion based on several repetitions of the stimulus. Data were collected while compensating for changes in fixational eye position (Snodderly and Gur 1995) and epochs perturbed by saccades were excluded (see METHODS). Upward histograms with light bars represent INC responses and downward histograms with dark bars represent DEC responses. *C*: same histograms as in *B*, converted to spatial dimensions with spatial position defined as the product of time and the velocity of the stimulus. The estimation of AR borders for the INC AR is illustrated for the forward (preferred) direction in the top half of *C*. The cumulative curve for the number of spikes fired is shown, along with dashed vertical lines that denote the intersections of least-squares lines fitted to the cumulative curve. Solid vertical lines represent AR borders as defined by 95% of the response between the intersections, distributed symmetrically around the center of mass. The same process (not shown) was carried out to define the DEC AR. The separation between the INC and the DEC centers (sep) was used to calculate the overlap index, OI. Note that the space histograms for backward motion (bottom half of *C*) are left-right reversed with respect to their time counterpart in *B* to reflect the actual spatial arrangement of the responses. The right (trailing) edge in time, denoted by the asterisk, is the left (leading) edge in space. The relative locations of INC and DEC ARs differ slightly in the forward and backward directions, due to small differences between INC and DEC response latencies (see RESULTS). Establishing the absolute position of the receptive field in the 2 directions requires taking the response latency into account, which is done in *D*. Correcting for the INC latency of 44 ms and the DEC latency of 55 ms for this cell shifts the histogram for forward motion to the left and the histogram for backward motion to the right, so that the estimate of spatial location of the ARs is consistent for the 2 directions.

$$RM = \frac{F1}{F0 - F0_{base}} \quad (2)$$

The mean ongoing firing rate with a uniform field of 1 cd/m² was used as a measure of baseline activity (F0_{base}).



The phase (in degrees) of response harmonics was calculated as phase = [angle(DFT) + π/2] · 180/π, where angle(DFT) = imag(log(DFT)) is the phase of the elements in a complex DFT vector. To eliminate discontinuities (jumps) due to phase wrapping, a simple “unwrapping” algorithm was applied. The algorithm minimized the SD of a set by adding 2π to each phase (1 at a time), re-calculating it, and then choosing the minimal SD.

Statistical analysis

Individual cells’ PSTHs were plotted with a 10-ms binwidth. Statistical comparisons were based on the following tests: for non-Gaussian-distributed variables (e.g., OI), the Mann-Whitney U test and the Wilcoxon matched-pairs signed-rank test; for Gaussian variables (e.g., AR width), t-test and paired t-test. Correlations between variables were calculated using the Spearman r or the Pearson r. Values reported for individual parameters are means ± SD. Analyses were done with custom software written in Matlab 5.3 (MathWorks).

RESULTS

A total of 228 V1 cells with receptive fields at 2–9° (mostly at 2–5°) eccentricity were studied. All cells were tested with sweeping bars, 101 cells were tested with flashing bars, and 114 were tested with sinusoidal gratings. Recording sites included a broad sample of all laminar locations.

We will refer to individual increment (INC)- and decrement (DEC)-responsive regions as activating regions (ARs) and the total region of space occupied by the activating regions as the classical receptive field (CRF). We describe first the spatial arrangement of the INC and DEC ARs within the CRF as measured with sweeping bars, along with information from flash responses. Then we consider the effects of fixational eye movements on the neuronal responses to sinusoidal gratings. Finally, we present a detailed analysis of the modulation of neuronal firing by gratings and its relationship to the spatial arrangements of the ARs.

Spatial organization of receptive fields

NEURONS WITH TWO OR THREE ACTIVATING REGIONS. Previous studies have shown that saccadic eye movements modify responses to sweeping bars (Gur and Snodderly 1997a; Gur et al. 1997; Snodderly and Gur 1995), even while compensating for the eye movements of fixation (image stabilization). Consistent with this observation, AR widths measured when all time periods were included (32 ± 16 minarc; “all data”) were inflated (P < 0.0001) compared with widths calculated from time periods ≥150 ms after any preceding saccade (28 ± 15 minarc, “no saccades”). Consequently, we base our spatial

FIG. 2. Distribution of overlap index (OI) for cells with 2 ARs. A–D: individual examples of CRF spatial maps. Each histogram is an average of several responses to a bar sweeping in the preferred direction with spatial position defined as the product of time and the velocity of the stimulus. Because the 10-ms time bin is scaled by the stimulus velocity, the spatial binwidth varies with the velocity. OI is displayed at the left of each set of histograms. A: simple cell 10982: INCw and DECw, 8 minarc; CRF, 24 minarc. B: simple cell 20681: INCw, 23 minarc; DECw, 26 minarc; CRF, 41 minarc. C: complex cell 28685: INCw, 21 minarc; DECw, 24 minarc; CRF, 29 minarc. D: complex cell 27766: INCw, 25; DECw, 24 minarc; CRF, 25 minarc. Bar width was 6 minarc in A and B, 4 minarc in C, and 5 minarc in D. E: distribution of OI for 211 cells with 2 ARs. □, simple cells; ■, complex cells; mean OI values for simple, △ (−0.04 ± 0.17) and complex, ▲ (0.82 ± 0.12) cells.

mapping results on the “no saccades” mode of data selection, combined with image stabilization, as the most straightforward method of correction for eye movements.

After each neuron's preferred orientation and color had been determined, receptive fields were mapped with increment and decrement bars sweeping forward and back across the CRF (Fig. 1). For some cells, spatially separated ARs could be defined by their responses to increment and decrement bars (Fig. 2, *A* and *B*), but for most cells, overlapping INC and DEC ARs were found (Fig. 2, *C* and *D*). An OI (see METHODS) was calculated that ranged from negative values for spatially separated INC and DEC ARs to 0 for immediately adjacent ARs to 1 for complete and symmetric overlap.

The distribution of the overlap index is shown in Fig. 2*E*, and it is obvious that there are two separate groups of cells. The cells with nonoverlapping ARs ($OI \leq 0.3$, $n = 33$, 14%) will be referred to as simple cells (Hubel and Wiesel 1962, 1968). Nine of these were tripartite simple cells with three ARs. In deference to common usage, cells with overlapping ARs ($OI \geq 0.5$, $n = 178$, 78%) will be called complex cells even though some of the original descriptions do not fit this category (e.g., Hubel and Wiesel 1962, Fig. 7). Although many laboratories have adopted weak response modulation to drifting gratings as the criterion for identifying complex cells (Skottun et al. 1991), we show later in RESULTS that many cells with spatially overlapping ARs have strongly modulated responses that are inconsistent with the expected behavior of complex cells.

CONTROL EXPERIMENTS. Because the measurement of AR and OI with moving bars is crucial to the results of this paper, we present evidence that our spatial mapping is not distorted by temporal effects. Although previous reports of receptive field measurements in monkey (Dow et al. 1981; Livingstone 1998; Schiller et al. 1976; Snodderly and Gur 1995) and cat (Peterhans et al. 1985) V1 have found that flashed or moving stimuli give comparable estimates of AR dimensions, the use of moving stimuli for spatial mapping raises two potential problems: 1) the relative positions of the INC and DEC ARs could be misjudged due to differences in response latency, and 2) prolongation of the response by temporal persistence could lead to an overestimate of the AR width and OI.

To examine the effects of response latency, we recorded responses to stationary flashing increment and decrement bars centered on the CRF. The flashed bars were the same width or slightly wider than the moving bars. Response latencies for increments were shorter than latencies for decrements (mean difference: 7 ± 4 ms; INC: 47 ± 12 ms; DEC: 54 ± 12 ms; $r = 0.92$; $P < 0.0001$). These differences will cause shifts in the apparent relative locations of INC and DEC ARs determined by the product of latency differences and stimulus velocities. Because the latency differences were small, correcting the OI for the differences on a cell-by-cell basis did not cause a significant change in the OI distribution (mean of *absolute* differences between initial and corrected OI: 0.07 , mean of signed differences: 0 , $P = 0.3$; Fig. 3*A*). Signed differences caused shifts either toward smaller or larger overlap depending on the relative AR arrangement, so the net effect was zero. We conclude that the effects of INC/DEC latency differences are small, and they lead to balanced increases and decreases of overlap that do not affect our conclusions about the OI distribution.

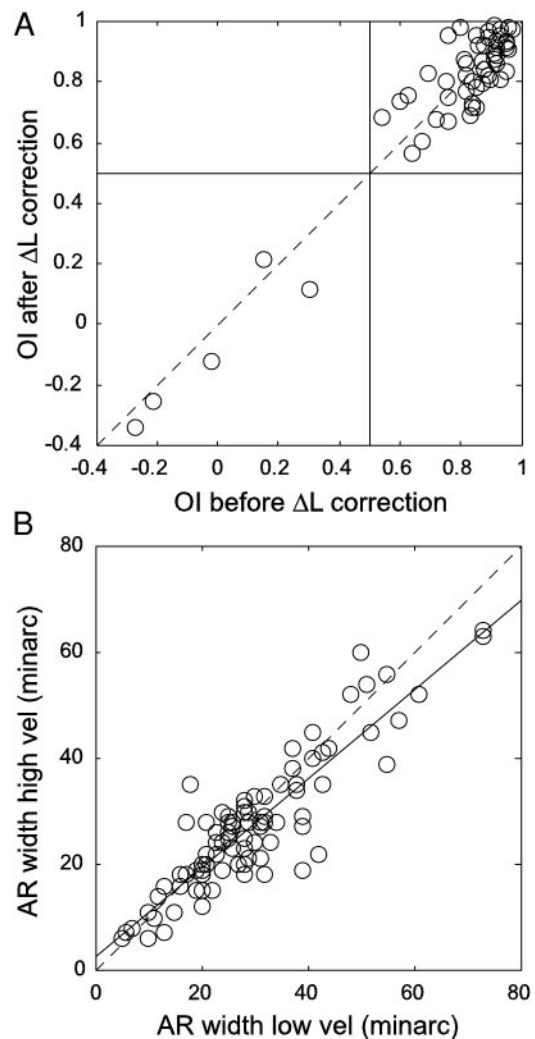


FIG. 3. Spatial mapping—control experiments. *A*: scatter plot of OIs before and after the correction for the INC/DEC latency difference for 56 cells for which both flash and grating data were available. ---, the line of equality. The latency differences shift the OI either toward higher or lower overlap, depending on a given RF spatial arrangement. That is, if a bar encounters the DEC zone first, and the DEC latency is longer than the INC latency, the measured overlap will be higher than the real one, and the correction will decrease it; alternatively, if the INC zone comes first, then the latency difference would cause underestimation of the overlap, and the correction will increase it. Note that in nondirectional cells, where OI could be reliably measured for both directions, INC/DEC latency differences produced a small OI discrepancy for the two directions of motion (e.g., complex cell shown in Fig. 1). The *absolute* OI difference was 0.07 ± 0.08 , but the signed difference was 0.0 ± 0.1 , ($P = 0.44$), because for any given AR arrangement the effect was opposite for the 2 directions. Using a OI for one direction and the latency difference, and assuming that the latency difference is the only reason for the observed discrepancy, one can predict the OI for the other direction. The good correspondence between the backward OI measured (0.79 ± 0.15) and the OI predicted from the forward OI and the latency difference (0.76 ± 0.19) showed that indeed the OI discrepancies for the 2 directions were mostly the result of the latency differences ($r = 0.82$, $P < 0.0001$). *B*: scatter plot of AR widths estimated with lowest and highest velocities in the set. ---, the line of equality; —, the least-squares fit (slope 0.84, $r = 0.9$, $P < 0.0001$). On average, the AR estimates for lower velocities (29 ± 13 minarc) were slightly larger than for higher velocities (27 ± 12 minarc; $P < 0.01$, $n = 92$).

The other factor that could introduce errors into OI estimation is the temporal persistence of the response. If the firing continued after the stimulus left the AR, it would blur the edge of the AR, inflating both AR width and OI. The higher the

velocity, the stronger would be the effect when translating from time to space. Our data do not conform to this prediction—the AR widths either remained nearly the same or decreased slightly with increasing sweep velocity from 3.5 ± 1.5 to $4.8 \pm 1.6^\circ/\text{s}$ (Fig. 3B). As a result, the OI decreased slightly when going from lower to higher velocity (0.73 ± 0.37 ; 0.66 ± 0.36 , $P < 0.01$). The responses to the highest velocities in the set had quite short durations (87 ± 42 ms, in the smallest ARs as short as 30 ms), providing little evidence for persistence of the response. Consistent with the view that receptive field dimensions measured with moving bars are not inflated, a recent report (Jones et al. 2001) found that CRF widths measured with drifting bars yield slightly smaller values than widths based on area summation criteria. Indeed we find that mean CRF and AR widths in our sample (Table 1) are either similar to (Born and Tootell 1991; Cumming and Parker 1999; Schiller et al. 1976; Vinje and Gallant 2002; Zhou et al. 2000) or smaller than (Foster et al. 1985; Li et al. 2000; Mazer et al. 2002; Rossi et al. 2001; Sceniak et al. 2001) measurements from other studies in monkeys made at comparable eccentricities.

Other data also are consistent with minimal persistence of V1 responses. Many cells fire short (≤ 50 ms) bursts of spikes in response to fast ($>10^\circ/\text{s}$) fixational saccades sweeping across a stationary stimulus (Snodderly et al. 2001) and in response to very fast flicker (Gur and Snodderly 1997b). Furthermore, responses to flashes usually do not last longer than the stimulus duration when latency is taken into account. Even cells that show some persistence in response to very brief flashes (e.g., “position/drift” cells) (Snodderly et al. 2001) yield very consistent measures of AR width with different stimulus velocities, which suggests that the responses to moving bars are cut short by inhibitory influences when the stimulus passes from the CRF into the surround. We suggest that in the presence of a constantly moving retinal image, this kind of invariance in translating time to space could be a useful feature for visual processing.

NEURONS WITH ONLY ONE ACTIVATING REGION. A third group of 17 cells (8% of our sample) responded to only one sign of contrast (monocontrast), either increment ($n = 10$) or decrement ($n = 7$). V1 cells responding to a single sign of contrast have been reported previously but they were only qualitatively described (Bullier and Henry 1980) or described as nonoriented with sustained firing (T cells) or oriented and predominantly direction selective (S1 cells) (Schiller et al. 1976). Our monocontrast cells appear to differ from the latter descriptions because they were all selective for orientation, but only 4/17 (24%) were direction selective (mean DI 0.3 ± 0.28).

COMPARISONS AMONG CELL TYPES. Figure 4 displays histograms of AR widths (*left*) and CRF widths (*right*) for the three cell types and Table 1 gives numerical summaries. For cells with more than one AR, the mean AR width was used. The *bottom row* of Table 1 combines data from all cells, including those that could not be assigned to layers. Considering the entire sample, simple cells' mean AR widths were significantly smaller than the mean AR widths of complex cells ($P < 0.0001$). INC and DEC AR widths were highly correlated for both simple and complex cells ($r = 0.88$, $P < 0.0001$). The AR widths of monocontrast cells were similar to the AR widths of simple cells.

Cells that could be assigned to individual layers were combined into upper (2/3), middle (all subdivisions of layer 4), and infragranular (5/6) groups because of the small number of simple cells in our sample. Simple cells had smaller ARs than complex cells in layer groups 4 and 5/6 ($P < 0.0001$). There were too few monocontrast cells in layer group 5/6 for comparisons, but they had smaller ARs than either simple cells ($P < 0.01$) or complex cells ($P < 0.0001$) in the upper layers 2/3 and smaller ARs than complex cells in layer group 4 ($P < 0.0001$).

The mean CRF widths of simple and complex cells did not differ significantly when cells from all layers were combined, in agreement with results from anesthetized monkeys (Foster et al. 1985). In the layer 4 group also, there was no significant difference between CRF widths of simple and complex cells. In the infragranular layers 5 and 6, simple cells' CRFs were much smaller than those of complex cells ($P < 0.01$). A group of very large complex cells (Fig. 4, *bottom panels*), all found in layer 6 (cf. Schiller et al. 1976), contribute to this relationship. We also found a small number of simple cells in the upper layers 2/3 with larger CRFs than those of the complex cells ($P < 0.01$). A larger sample of simple cells will be needed to determine whether this is a general pattern.

In addition to moving stimuli, a subset of cells ($n = 101$) were tested with stationary flashing bars. Note that because we used both light (increment) and dark (decrement) stimuli, the terms “increment/decrement” are not equivalent to the “ON-OFF” terminology because an INC AR may give an OFF response to extinguishing of a decrement stimulus and a DEC AR will respond to the *onset* of a decrement stimulus. In agreement with previous findings (e.g., Dean and Tolhurst 1983; Hubel and Wiesel 1962, 1968), most simple cells (7/9) gave only ON or OFF responses at each spatial location, while most complex cells responded in an ON-OFF fashion to both increment and decrement flashes. Monocontrast cells ($n = 9$) gave only on responses to stimuli of the appropriate contrast.

Monocontrast cells' responses to flashes were more sus-

TABLE 1. *Dimensions of activating regions and classical receptive fields*

Layer Group	AR, minarc			CRF, minarc		
	Simple	Complex	Monocontrast	Simple	Complex	Monocontrast
2/3	22 ± 3 (5)	23 ± 10 (49)	7 ± 2 (5)	48 ± 11 (5)	26 ± 12 (49)	7 ± 2 (5)
4	12 ± 7 (18)	28 ± 11 (74)	18 ± 8 (7)	29 ± 16 (18)	32 ± 13 (74)	18 ± 8 (7)
5/6	8 ± 5 (9)	49 ± 33 (29)	19 ± 12 (3)	19 ± 12 (9)	56 ± 33 (29)	17 ± 11 (3)
All cells	13 ± 8 (33)	31 ± 18 (178)	14 ± 8 (17)	29 ± 16 (33)	35 ± 21 (178)	14 ± 8 (17)

Numbers of cells are in parentheses. 1/33 simple, 26/178 complex, and 2/17 monocontrast cells were not assigned to layers but were included in the statistics for all cells. Values are means \pm SD. AR, activating region; CRF, classical receptive field.

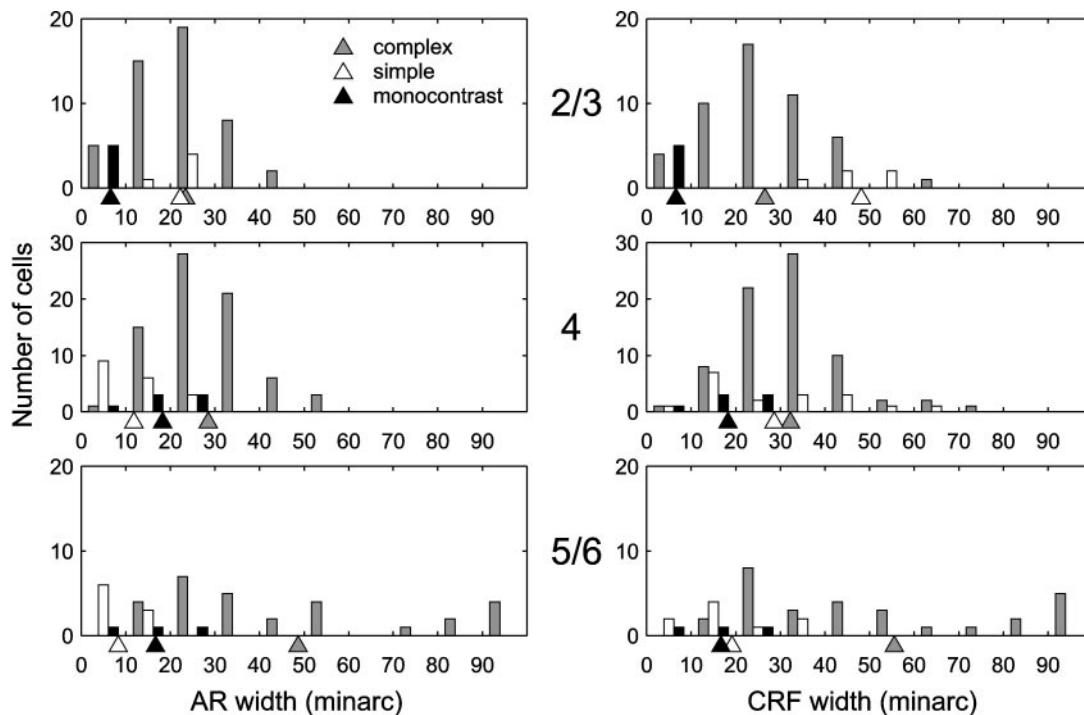


FIG. 4. The distributions of AR and CRF widths within groups of cortical layers. *Top*: layers 2 and 3. *Middle*: all subdivisions of layer 4. *Bottom*: infragranular layers 5 and 6. *Left*: distributions of AR widths for all 3 cell types. Triangles beneath the abscissas denote mean AR widths. *Right*: distributions of CRF widths for the same cells. CRF widths for monocontrast cells are identical to AR widths. Triangles beneath the abscissas denote mean CRF widths. Bin width: 10 minarc.

tained than the responses of simple and complex cells. A transiency index (TI) (Snodderly et al. 2001) that ranged from near zero for perfectly sustained responses to 1 for very transient responses was significantly smaller ($P < 0.05$) for monocontrast cells (0.12 ± 0.33) than for simple cells (0.40 ± 0.41) and complex cells (0.40 ± 0.33). This temporal difference in the response of the monocontrast cells, along with the small sizes of their ARs (Table 1) reinforces the idea that they should be treated as a separate group.

Almost all cells (50/53) tested with flashing bars of increasing widths exhibited strong side inhibition with a response reduction of $\geq 50\%$ as the stimulus was extended beyond the CRF.

Effects of eye movements on grating responses

It was apparent from inspecting the records that fixational eye movements considerably affect neuronal responses to gratings (Fig. 5). Almost all saccades and some slower eye movements were followed by spurious firing after a variable delay. For the complex cell illustrated in Fig. 5, responses to the drifting grating during stable fixation appeared mostly in the second half of the stimulus cycle, while eye movements shifted the responses in time or eliminated them.

To analyze effects of eye movements, we used the stimulus combination of spatial frequency and window size that evoked maximal RM. Each behavioral trial was split into segments corresponding to one temporal cycle of the grating. To quantify the effects of eye movements, the relative modulation (RM) was calculated (see METHODS) using two different modes of data selection as shown in Fig. 5A: 1) accepting all segments (“all”) or 2) automatically detecting fixational saccades by a velocity

criterion and discarding segments following saccades within 250 ms (“no saccades”). Segments affected by saccades were discarded because our compensation for eye movements (image stabilization) had too large a delay to correct for saccades (see METHODS). Even during the slower movements of the intersaccadic intervals, noise in the eyetracker signal, small calibration errors, and small deviations from linearity cause position errors of a few minutes of arc that are difficult to eliminate. These residual position errors in image stabilization result in phase jitter of the retinal image of sinusoidal stimuli and corresponding jitter of the phases of the neuronal responses (cf. Bridge and Cumming 2001). To correct for the phase jitter, an additional measure of the relative modulation was calculated by dividing the “no saccades” data into segments corresponding to one temporal cycle of the grating and averaging the RMs of individual segments. This calculation is equivalent to phase alignment in the frequency domain (“aligned”). In principle, alignment could be done in the time domain, but that would produce erroneous results when applied to modulated responses that span adjacent temporal cycles. Figure 5D shows how RM increased as the effects of eye movements and the accompanying time jitter in the response were progressively reduced.

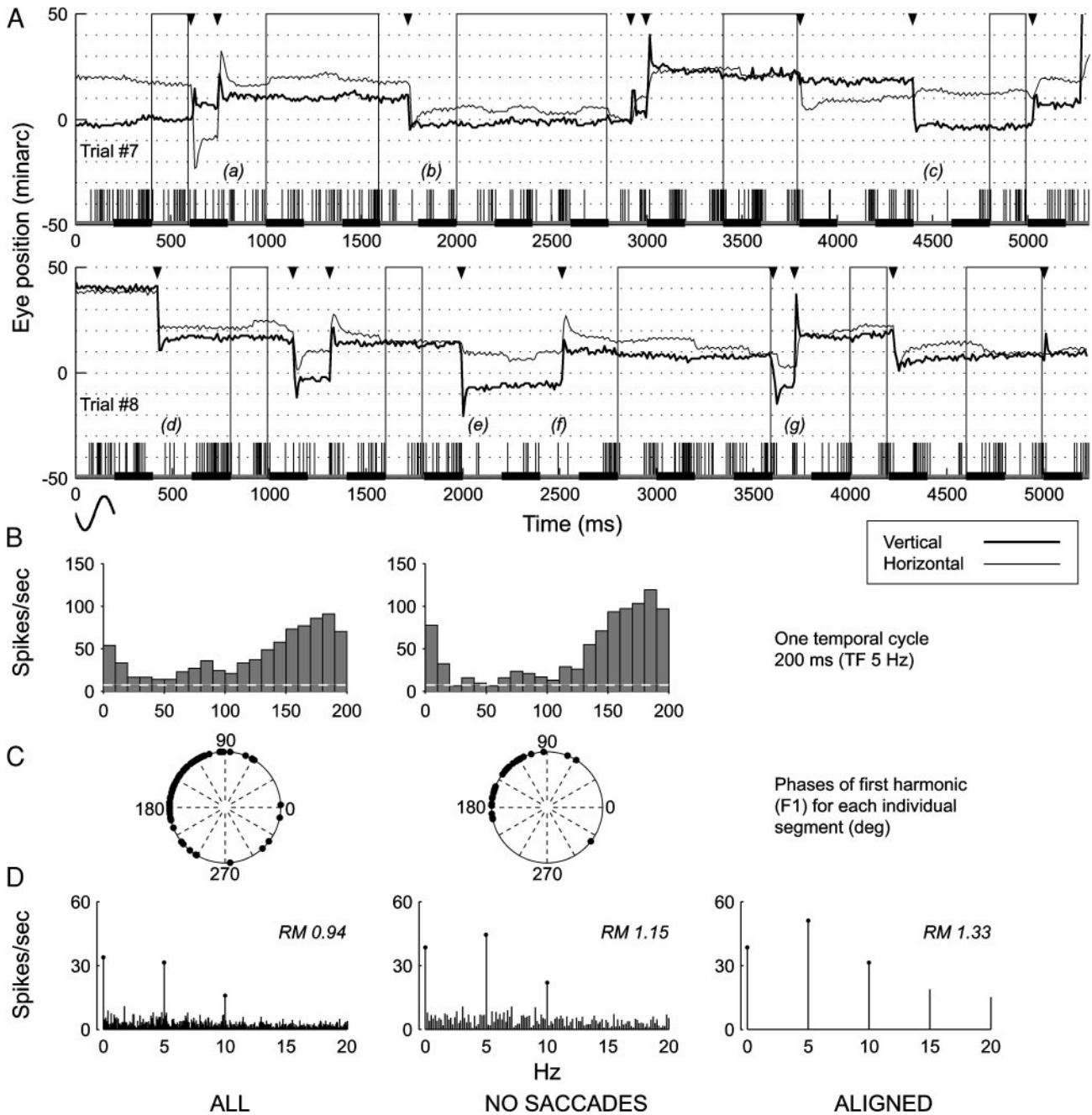
As data selection became more stringent, the distributions of RM shifted toward more modulated values (Fig. 6, going from *top* to *bottom*). Simple cells and complex cells were similarly affected by saccades (Table 2). Elimination of data segments affected by saccades increased the mean RM by 22% for simple cells and by 29% for complex cells (Fig. 6, *middle*). Phase alignment increased the mean RM of simple cells by an additional 22% and of complex cells by an additional 42% (Fig. 6, *bottom*). The overall effect of removing both saccade

influences and phase jitter was an increase in RM of 0.55 units (49%) for simple cells and 0.51 (84%) for complex cells. Thus RM increased by almost the same amount for both cell types but by a larger percentage for complex cells because they had a lower RM before data selection. Note that selecting data segments with minimal effects of saccades and then performing phase alignment resulted in a $RM > 1$ for all simple cells, like the results from anesthetized animals. However, the same procedure resulted in 53/93 (57%) of the complex cells having an $RM > 1$, which distinguishes them from the complex cells described in anesthetized preparations.

Phase alignment to correct for eye movements has been previously employed (Carandini et al. 1997; Cumming et al. 1999), and our results suggest that it helps to minimize the effects of stabilization errors. One would predict that stabiliza-

tion errors should produce phase dispersion (SD of the phase of F1 across response cycles) that is greater for cells with smaller CRFs and for cells with higher optimal spatial frequencies. Consistent with this prediction, we found that for complex cells, phase dispersion of the “no saccades” data were negatively correlated with CRF width ($r = -0.29, P < 0.005$) and positively correlated with optimal spatial frequency ($r = 0.52, P < 0.0001$). Also, as would be expected, the increases in the RM values for complex cells produced by aligning the segments were positively correlated with spatial frequency ($r = 0.5, P < 0.0001$). Trends were the same for simple cells, but the sample was too small to reach statistical significance.

These results suggest that RM values derived from the “no saccades” analyses are underestimates of the true values, especially for cells with small receptive fields or high optimal



spatial frequencies. However, the RM values derived from analysis of the aligned segments may be overestimates if there are significant phase shifts in the neuronal responses due to other factors, such as intrinsic temporal properties of the neurons (Garcia-Perez 1999). To encompass the range of values that are our best estimates of the properties of the neurons, we present the summary data with results based on both methods of analysis.

Analysis of responses to gratings

When studying each neuron, several stimulus combinations of window size and spatial frequency were presented. For comparison with previous studies, the amplitude of the response harmonics F0 and F1 to drifting gratings were calculated, and RM was calculated for the stimulus condition generating the maximal harmonic of the entire set. If the maximal harmonic in the set was F0, RM was <1 , and if the maximal harmonic was F1, RM was >1 , which is the traditional criterion to distinguish simple cells from complex cells based on sinusoidal stimulation (De Valois et al. 1982; Skottun et al. 1991).

In Fig. 7, typical responses to gratings are illustrated for a simple cell and three complex cells. To be conservative, the data for the figure have been analyzed in the “no saccades” mode. The simple cell (A) and the first complex cell (B) exhibit properties characteristic of simple and complex classes found in anesthetized cats and monkeys. The simple cell response was highly modulated, whereas the complex cell was almost unmodulated. Many readers would expect this result, based on the spatial overlap of the INC and DEC ARs (Skottun et al. 1991). However, for the other complex cells (C and D) with similar OIs, drifting gratings evoked strong F1 modulation at the stimulus temporal frequency (5 Hz). Strong modulation was relatively common among complex cells, and we show later in RESULTS that the strength of the modulation was not related to the spatial receptive field organization.

Responses to counterphase gratings (*middle left* and *middle right*) were similar to those described for anesthetized preparations: the simple cell responded once during a stimulus cycle,

whereas the complex cells responded twice per cycle, like typical complex cells (De Valois et al. 1982). Note that the presence of a large, pseudolinear F1 harmonic (5 Hz) in the response of the complex cells C and D to a drifting grating is nevertheless associated with a large nonlinear F2 harmonic (4 Hz) in response to the stationary, counterphase grating.

Distributions of response modulation to drifting gratings

A total of 114 cells (93 complex, 16 simple, and 5 mono-contrast) were studied with drifting sinusoidal gratings. When choosing the stimulus configuration for analyzing the responses to drifting gratings we used two criteria. One was the stimulus evoking the largest F0 or F1, as described in the preceding text. We refer to this as the stimulus evoking the maximal harmonic. Because the relative modulation may be a more important means of transmitting information than the maximal harmonic (Reich et al. 2001), we also analyzed responses to the stimulus producing the maximal RM.

For the examples of Fig. 7, and for 75% of simple cells and 57% of complex cells, the stimulus parameters evoking the maximal harmonic and the maximal RM were the same. For the rest of the simple and complex cells ($n = 44$), choosing the stimulus condition that produced the maximal RM reduced the amplitude of the maximal harmonic (F0 or F1) by 23 ± 19 spikes/s, or $34 \pm 17\%$, but increased the mean RM by $47 \pm 30\%$.

The value of RM was a function of both the choice of the stimulus and the mode of correction for eye movements (Table 3). In the most extreme two-way comparison, the mean RM assigned to complex cells for a stimulus eliciting the maximal RM analyzed with phase alignment of the response was nearly twice as large as the mean RM for a stimulus eliciting the largest single harmonic with only elimination of saccades.

Figure 8 shows histograms illustrating the effects of these variables on RM values. For each condition, there was considerable overlap between the RM distributions of simple and of complex cells. Using the maximal harmonic as the traditional criterion for choice of stimulus and the conservative “no saccades” mode of data analysis (Fig. 8A), many complex cells

FIG. 5. Effects of eye movements on responses to gratings: Data selection and analysis. A: responses of a complex cell to a drifting sinusoidal grating during 2 behavioral trials of ~ 5 -s duration (*cell 04983*; trials: 7, 8; OI: 0.96, CRF: 24 minarc). Eye position (thick line, vertical; thin line, horizontal) is plotted along with the spike train, which is indicated by short vertical lines underneath the eye-position traces. Fixational saccades in these records often appear to have overshoots that are actually pairs or clusters of saccades. These apparent transients are reduced or absent in voluntary saccades (see Fig. 2 in Snodderly 1987). The abrupt saccadic clusters do not intrude on the analyses of neuronal activity during the drift periods. The stimulus was a sine wave grating of 1 cycle per degree (cpd) spatial frequency drifting at 5-Hz temporal frequency within a window of 33 minarc. The trial is divided into segments corresponding to the temporal cycles of the stimulus. Each 2nd temporal cycle of 200-ms duration is marked by a short, thick horizontal line under the spike train. Black inverted triangles above the position traces denote saccade occurrences. Data selection modes are designated as follows: “all,” all data were used; “no saccades,” only trial segments with no saccades in the immediately preceding period of 250 ms were accepted. These epochs are framed by boxes formed by thin solid lines. One such frame includes the period from 1,000 to 1,600 ms (3 cycles) in the *topmost trial*. Examples of fixational saccades’ effects on neuronal discharge are labeled with letters a–g below the eye position traces. Note that during periods of relatively stable fixation, the response spanned the first 20 ms and the last 80 ms of a temporal cycle (i.e., the response phase is $\sim 150^\circ$). However, almost every saccade resulted in a spurious burst (e.g., a and b), response displacement (e.g., d, e, and g) or in a missed response (e.g., c and f). B: cycle-averaged histograms computed over segments accumulated in “All” (*left*) and “No saccades” (*right*) data selection modes. Note the reduction of the unmodulated component F0 and the increase of the F1 component in the “No saccades” histogram. Dashed horizontal lines indicate the mean ongoing firing rate (8.5 spikes/s). C: phase plots of the F1 response harmonic for individual stimulus cycles for “All” (*left*) and “No saccades” (*right*) data selection modes. Each dot represents the phase of one response cycle. Note that although there is less phase dispersion in “No saccades” data (SD: 46°) as compared with “All” data (SD: 54°), a significant jitter still persists. D: harmonic analysis of the data. “All” data (*left*) and data selected for “No saccades” (*middle*), compared with a phase-aligned spectrum (*right*, “Aligned”). F0 (0 Hz), F1 (5 Hz), and F2 (10 Hz) harmonics are marked by dots at the end of corresponding amplitude lines. Note the increase of RM values (*top right corner* of each graph) from “All” to “No saccades” to “Aligned” spectra.

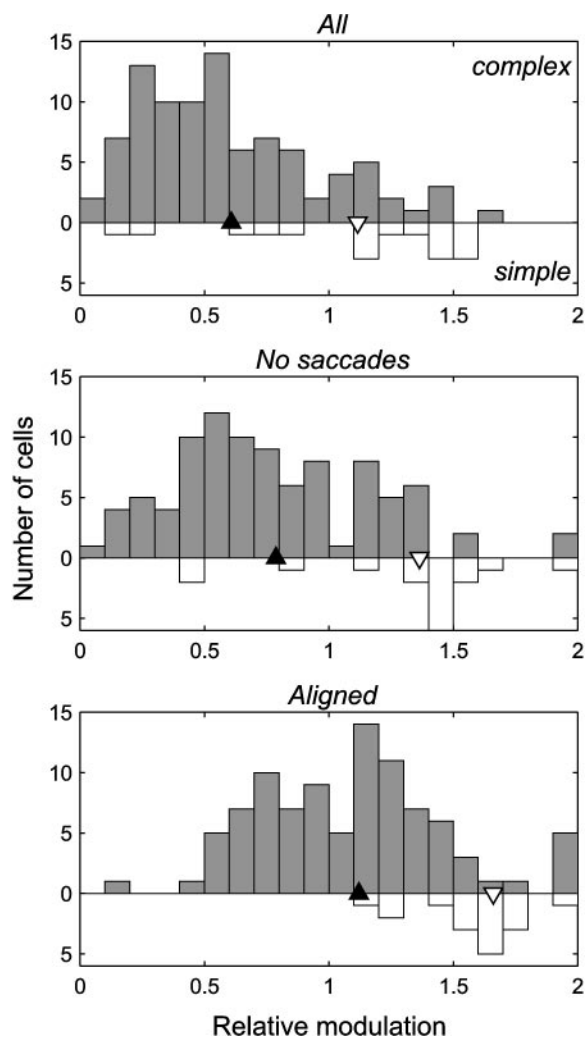


FIG. 6. Effects of eye movements and data selection on relative modulations (RM) distributions. Each panel shows the RM distribution for complex and simple cells for 1 of the modes of data selection. In this and all subsequent population figures, ■, complex cells; □, simple cells; ▲ and ▽, the mean RMs of complex and simple cell populations for a given mode, respectively.

showed a substantial degree of modulation and 14% had $RM > 1$. Most simple cells (69%) had $RM > 1$, although for five cells, $RM < 1$. When response phase was aligned (Fig. 8B), both complex and simple cell responses were more modulated; 37% of complex cells had $RM > 1$ and 87% of simple cells had $RM > 1$. Selecting the stimulus for maximal RM (Fig. 8, C and D) increased the number of complex cells with $RM > 1$ to 26% and had an especially large effect on the complex cells when analyzed with phase alignment: more than half the complex cells (57%) had $RM > 1$ and all simple cells had $RM > 1$ (Fig. 8D).

These results suggest an explanation for the discrepancy in the literature between the small percentage (7–22%) (Dow 1974; Foster et al. 1985; Hubel and Wiesel 1968; Schiller et al. 1976; see also Conway 2001) of neurons in V1 designated as simple by spatial mapping and the relatively large percentage (40–60%) (De Valois et al. 1982; O'Keefe et al. 1998; Sceniak et al. 1999, 2001) found by relative modulation. By relative modulation criteria 14–37% of complex cells identified by spatial mapping would be considered simple cells, depending on the mode of analysis. Because complex cells constitute the

large majority of V1 cells (78% of our sample), the use of $RM > 1$ as a criterion for identifying simple cells will result in a mixed population, a large fraction of which are complex cells by spatial criteria.

Thus in our sample of V1 cells, RM would not be a reliable criterion for predicting the spatial organization of the CRF. Depending on the mode of analysis and stimulus conditions (eliciting the maximal harmonic or the maximal RM), 13–31 to 0–19% of the simple cells and 14–37 to 26–56% of the complex cells would be grouped with other cells with unlike spatial receptive fields.

We have not discussed the responses of monoflash cells to drifting gratings because they were weak and variable, though well modulated (mean RM: 1.56). Even with stimuli selected for the maximal harmonic, the mean response amplitude was only 18 spikes/s (cf. complex cells: 54 spikes/s, simple cells: 36 spikes/s).

Relative modulation versus spatial organization

Scatter plots illustrating the relationship between the OI and the value of RM for each cell are shown in Fig. 9. For both maximal harmonic and maximal RM stimulus conditions, there was no statistically significant correlation, although there may be a weak negative relationship for the maximal harmonic condition. The weak relationship between INC and DEC overlap and RM reinforces the conclusion that factors other than spatial overlap must exert strong influences on the modulation behavior of the neurons.

Two additional parameters that we measured do not appear to influence the modulation behavior of the cells. There was no correlation between RM and the CRF width in all conditions for both simple and complex cells (data not shown). Also, no significant correlation was found between RM and the transiency, TI, of responses to flashes.

Responses to counterphase gratings

Fifty-three complex cells were tested with counterphase gratings. For 25 cells, the spatial frequency of the counterphase grating was the same as the spatial frequency selected for one or both stimulus conditions used with the drifting grating; for the rest, the mean difference between the spatial frequency of the counterphase grating and the spatial frequency of the drifting grating (in either stimulus condition) was < 1 cpd.

Forty-seven of 53 complex cells responded to counterphase gratings with an F2 harmonic greater than the F1 harmonic and $\geq 40\%$ of the F0 harmonic. Of the remaining six cells, five had little modulation and one exceptional complex cell had a strong

TABLE 2. RM distributions for different data analysis modes (maximal RM stimulus condition)

Data Analysis Mode	RM	
	Simple cells (16)	Complex cells (93)
All segments	1.11 \pm 0.45	0.61 \pm 0.36
No saccades	1.36 \pm 0.49	0.79 \pm 0.43
Aligned F1 phase	1.66 \pm 0.40	1.12 \pm 0.46

Values are mean \pm SD. Numbers of cells are in parentheses. RM, relative modulation; F1, first harmonic.

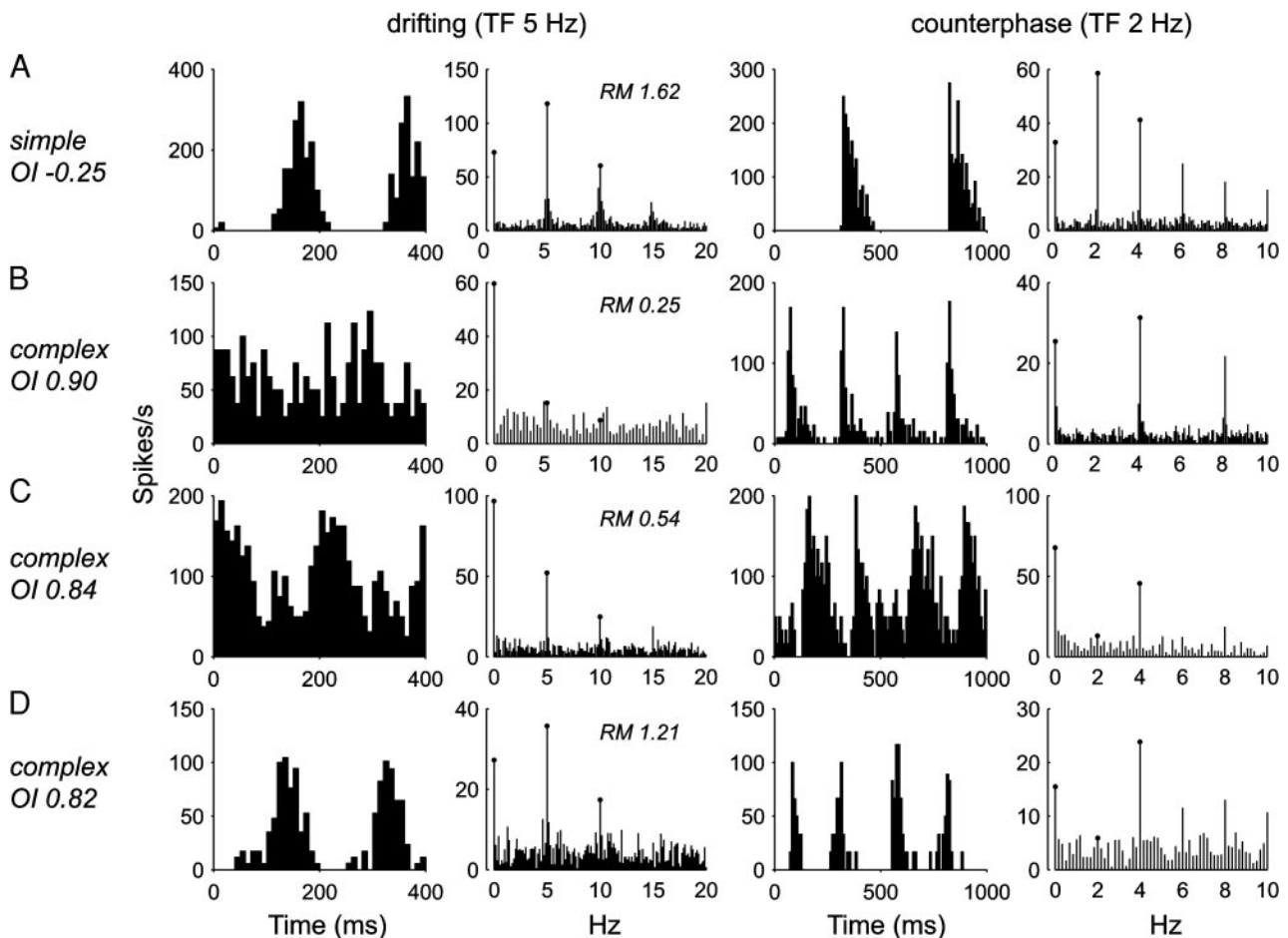


FIG. 7. Simple cell and complex cell modulation behavior. Each row represents responses of a cell, labeled with the cell type and overlap index, OI. *Left*: cycle-averaged PSTH (2 temporal cycles with 10-ms binwidth) for a grating with nearly optimal spatial parameters, drifting at 5 Hz. *Middle left*: the amplitudes of the response harmonics and the RM. *Middle right*: the PSTHs for the same grating centered on the receptive field and temporally modulated with a 2-Hz square wave (counterphase flicker). *Right*: the amplitudes of the response harmonics for the counterphase flicker. *A*: responses of a simple cell (10982, ongoing discharge, 0 spikes/s; CRF, 24 minarc; INCw, 8 minarc; DECw, 8 minarc). *B*: unmodulated complex cell 24884 (ongoing discharge, 0.01 spikes/s; CRF, 37 minarc; INCw, 32 minarc; DECw, 37 minarc). *C*: moderately modulated complex cell 03984 (ongoing discharge, 5 spikes/s; CRF, 36 minarc; INCw, 34 minarc; DECw, 32 minarc). *D*: very modulated complex cell 16885 (ongoing discharge, 0 spikes/s; CRF, 28 minarc; INCw, 24 minarc; DECw, 27 minarc).

F1 response. The prevalence of even harmonics in cells with overlapping INC and DEC ARs suggests that the responses to counterphase gratings could prove more consistent as counterparts for spatial mapping than the degree of modulation to drifting gratings.

Only four simple cells were tested with counterphase gratings, so we cannot draw conclusions about population behavior.

Spatial frequency selectivity

For 102 cells (88 complex and 14 simple), data were collected with gratings of several spatial frequencies covering a mean range of 2.2 ± 0.8 octaves. Spatial frequency selectivity curves were analyzed using an automated procedure: for each curve, the maximum response was normalized to 1 and if the response at low, high, or both ends of the spatial frequency range was $<71\%$ of the maximum ($1/\sqrt{2}$), the curve was considered as having a cutoff frequency. For 51% of the cells, we reached both high- and low-frequency cutoffs or found no

clear attenuation with spatial frequency. Thus for half of our sample, we had quantitative confirmation that we operated in a spatial frequency range that was near the optimum for the cell. For the rest of the cells, we reached one cutoff, but we did not obtain data for enough spatial frequencies to cover the cell's entire bandwidth. We only had time to collect data around the spatial frequency that we judged qualitatively to elicit the strongest response. To confirm that for this half of the sample we used spatial frequencies that were in a nearly optimal range, we compared the distributions of the spatial frequencies used for the two half-samples and the resulting complexity indices (see following text). The two groups did not differ significantly ($P > 0.2$ for both comparisons), so data from all cells were combined.

Spatial frequencies for maximal harmonic and maximal RM stimulus conditions are shown in Fig. 10A. Simple and complex cells share the same distribution pattern, with a mode at 1 cpd and mean ~ 1.5 cpd. The mean is slightly lower than the values reported for anesthetized monkeys at comparable eccentricities (cf. 2.2 cpd in Foster et al. 1985; 2.2–3.2 cpd in De

TABLE 3. RM for stimuli producing the maximal harmonic or the maximal RM

Response Criterion for Choice of Stimulus	RM, No Saccades		RM, Aligned F1 Phase	
	Simple (16)	Complex (93)	Simple (16)	Complex (93)
Maximal F0 or F1	1.21 ± 0.46	0.60 ± 0.41	1.51 ± 0.31	0.92 ± 0.45
Maximal RM	1.36 ± 0.49	0.79 ± 0.43	1.66 ± 0.40	1.12 ± 0.46

Values are means ± SD. Numbers of cells are in parentheses.

Valois et al. 1982). However, differences in experimental conditions, including the lower stimulus luminance in our experiments, may be responsible for these minor discrepancies.

It has been suggested that modulated responses of complex cells could result from “too-low spatial frequency” of the grating (Skottun et al. 1991). This was clearly not the case in our experiments. For 74/93 complex cells, spatial frequencies for maximal harmonic and maximal RM conditions either coincided or the spatial frequency that elicited the maximal RM was *higher* than the spatial frequency eliciting the maximal harmonic.

Complexity index (CI)

Distributions of the number of grating cycles within the CRF (*complexity index*, CI) (Glezer et al. 1980) for both the maximal harmonic and maximal RM conditions are shown in Fig. 10B. The means of the distributions do not differ, so in the remainder of RESULTS, we will use the maximal harmonic condition analyzed in the “no saccades mode” for comparisons with data of other authors.

The idea behind the complexity index is that it may reveal the presence of preceding “subunits.” We did not find evidence for multiple subunits in most complex cells, unlike complex

cells described in some earlier papers (Movshon et al. 1978; Pollen and Ronner 1983). Half of our complex cells, including those with RM >1, had a CI ~0.5, so that a half cycle of the grating filled the CRF (Fig. 10C), and more than two-thirds of the cells had a CI ≤1. The mean CI was not different for simple cells (0.80 ± 0.68) and complex cells (0.76 ± 0.42), unlike the situation in cat, where complex cells had larger CIs than simple cells and most cells had CI ≥1 (Glezer et al. 1980). Values of CI reported for anesthetized monkeys are also larger than we have found (Foster et al. 1985). In fact some cells in our sample had values of CI <<0.5 that may be due to strong inhibitory surrounds that encroach on the CRF center (Snodderly and Gur 1995), and conceal weak receptive field regions when narrow single bars are used as probes (Carandini et al. 1999; De Valois et al. 2000; Glezer and Gauzelman 1997). The absence of multiple (>3) spatial lobes in our sample of simple cells is also consistent with concealment by powerful inhibitory influences.

Spatial frequency and window size interactions

We also calculated how many grating cycles were optimal for a given condition. This measure is different from CI: it is the number of cycles that fit a grating window, not the CRF. For complex cells, 1.0 ± 0.8 cycles of a grating were optimal, and for simple cells it was 1.6 ± 1.3. These relationships are illustrated for the 40 complex cells nearest the mode of the CI distribution in Fig. 10C.

In 42/54 cells for which data with different grating windows were collected, window size had a clear effect on the response amplitude. The ratio of the most effective window widths to CRF widths was similar for maximal harmonic (1.5) and maximal RM (1.6) conditions. In most cases, window sizes slightly wider than the bar-responsive regions were most effective, although for several cells, windows smaller than the

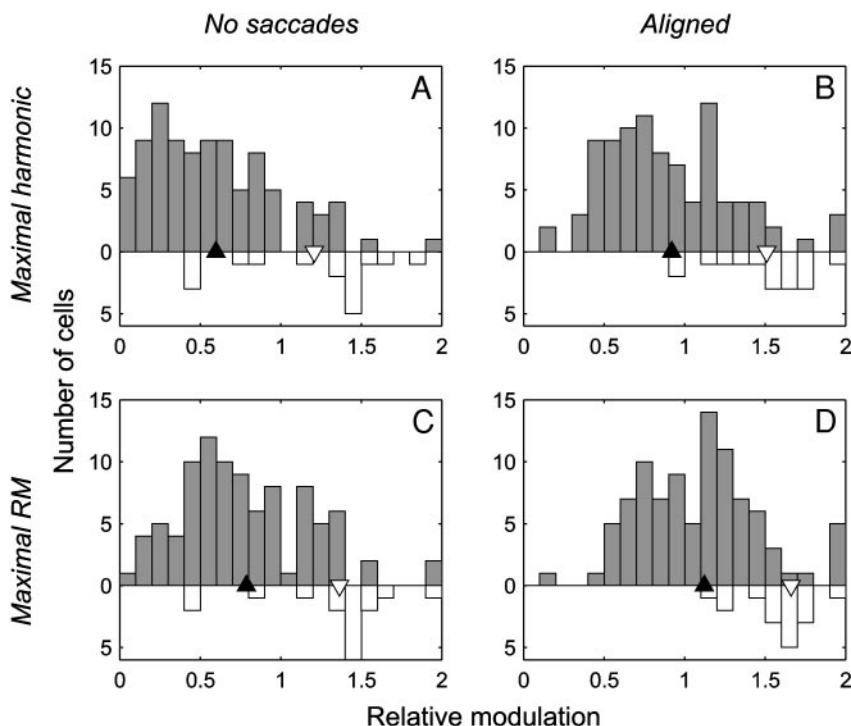


FIG. 8. Relative modulation distributions for different stimulus conditions and analysis modes. ■, complex cells; □, simple cells. *Left*: “no saccades” analysis mode. *Right*: “aligned” analysis mode. *Top*: RM distributions for stimulus conditions eliciting the maximal harmonic F0 or F1. *Bottom*: RM distributions for stimulus conditions producing maximal RM. See Table 3 for means of the distributions.

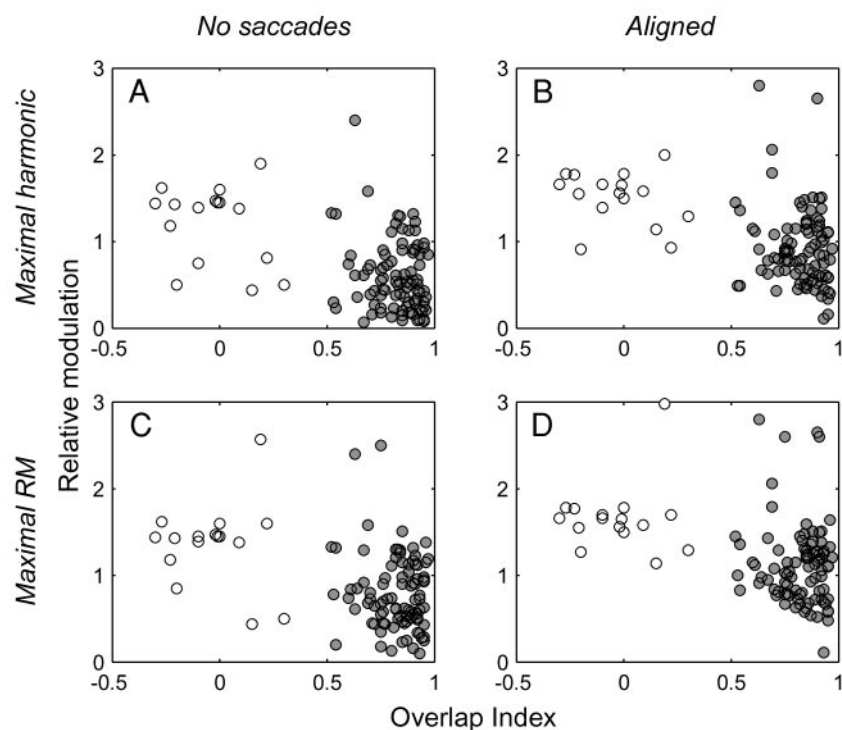


FIG. 9. Comparison of OI and RM. ○, simple cells; ●, complex cells. *Left*: “no saccades” analysis mode; *right*: “aligned” mode. *Top*, A and B: maximal harmonic condition. Correlation coefficients for complex cells, $r = -0.2$, no saccades; $r = -0.18$, aligned; for simple cells, $r = -0.26$, no saccades; $r = -0.26$, aligned. *Bottom*, C and D: maximal RM condition. Correlation coefficients for complex cells, $r = -0.16$, no saccades; $r = -0.11$, align; for simple cells, $r = -0.07$, no saccades; $r = 0.09$, align. $P > 0.05$ in all cases.

CRF were required to obtain a response to drifting gratings because of strong side inhibition. These results are in agreement with Born and Tootell (1991), who found that inhibition could occur within the bar-responsive region as well as beyond the bar-responsive region, as would be expected from a receptive field model with overlapping center and surround mechanisms (Sceniak et al. 2001).

For the subset of 21 complex cells assigned to layers 2/3, the number of grating cycles within the window was 1.2 ± 0.6 , similar to that reported for supragranular complex cells of anesthetized monkeys (1.3 ± 0.6) (Born and Tootell 1991). Moreover, side inhibition was common in other layers (cf. Sceniak et al. 2001): in 27/42 cells, the response declined when the grating width was extended 1.2–4 times beyond the CRF. These results are in agreement with the conclusion that most neurons in V1 are not tuned to extended periodic stimuli but rather to spatially restricted object boundaries (Born and Tootell 1991; Sceniak et al. 2001; von der Heydt et al. 1992).

For many complex cells, the harmonic content of the response strongly depended not only on the spatial frequency but also on the spatial window of the grating. An example of the spatial-frequency–window-size interaction for a complex cell is shown in Fig. 11A. Increasing spatial frequency with a fixed window, or increasing window size at a fixed spatial frequency, transformed the response from a frequency doubled to an F1-modulated response. The responses of several complex cells were similarly affected by increasing the grating width beyond the CRF borders, thus demonstrating that the surround may not only suppress or facilitate cells’ responses but also have a strong effect on the form of the response. The surround influence was particularly powerful for 10 complex cells and 1 simple cell (of 54 cells tested), resulting in different window widths for max-

imal harmonic and for maximal RM stimulus conditions. Taken together, these data suggest that V1 neurons can be very context-sensitive and produce a variety of responses depending on stimulus parameters.

The conditions under which frequency doubling occurs is another line of evidence that high RM values in complex cells did not result from too low a spatial frequency. Frequency doubling was defined as $F2 > 0.85 \cdot F1$ (where 0.85 is twice the $F2/F1$ ratio for a half-rectified sine function). We observed this feature in response to drifting gratings of low spatial frequency in 28/93 complex cells (and 1 simple cell). However, in 24 of 28 cells, RM was *higher* in response to higher spatial frequencies ($n = 19$) and/or another window size of the grating ($n = 5$). Most of these cells had significant F1 modulation: 16/24 cells had maximal RM > 0.5 and 3 had maximal RM > 1 , “no saccades” mode. Another example of a cell whose RM decreased as spatial frequency was lowered is presented in Fig. 11B. In response to a grating of high spatial frequency, this cell was modulated at the grating’s temporal frequency (*1st row*). With decreasing spatial frequency, the second harmonic appeared in the response (*2nd and 3rd rows*), and prevailed over the fundamental. Thus low spatial frequencies resulted in frequency doubling (F2) modulation and *lower RM* values.

Frequency doubling in response to a drifting grating occurred in complex cells with a combination of low spatial frequency and a small window. The mean number of cycles fitting the window was only 0.3 ± 0.15 , the grating window covered only part of the CRF in half the cells, and the mean CI in the stimulus condition eliciting strongest doubling was 0.34 ± 0.17 , roughly half the value of the CI for maximal RM and maximal harmonic conditions. Therefore we suggest that frequency doubling is evoked by temporal variation in the flux in the CRF. When only a small fraction of the grating cycle

(<0.5) is exposed to a CRF that responds to both light increments and decrements, two peaks per one temporal cycle (1 for the dark and 1 for the bright lobe of the grating) will be present in the response.

DISCUSSION

Simple and complex cells

In this paper, we have shown that spatial mapping distinguishes three cell types: simple, complex, and monococontrast. We have made the first quantitative measurements of the spatial overlap of INC and DEC ARs and the relationship to CRF width in V1 of alert monkeys. For cells with two ARs, the distribution of OI consists of two separate parts, corresponding to simple and complex cells. We found that the majority of V1 neurons were complex cells with overlapping INC and DEC regions (78%), while simple cells comprised only 14% of the whole sample. Previous work in anesthetized animals has also shown a bimodal distribution of the OI, with only 4% common range (monkey, Schiller et al. 1976) or completely dichotomous (cat, Heggelund 1986). This consistent pattern demonstrates the robustness of spatial mapping as a criterion for identifying neuronal classes in both anesthetized and alert animals, provided that eye movements are taken into account.

We have also compared spatial mapping and sinusoidal stimulation of the same neurons. The results show that the well-established spatial nonoverlap/overlap (simple/complex) dichotomy is not equivalent to classification by modulation to drifting gratings. The most obvious problem with using relative modulation as a criterion is that many complex cells are grouped together with simple cells. This practice obscures the laminar distribution of the simple cells. Although the use of relative modulation as a criterion results in placing presumed simple cells rather uniformly throughout the cortical layers (Sceniak et al. 1999, 2001), Hubel and Wiesel (1968) originally reported that simple cells of monkey V1 were unevenly distributed with the majority found in the middle layers. Bullier and Henry (1980) later presented evidence that these simple cells were predominantly driven by the magnocellular input from the lateral geniculate nucleus. Consistent with this conclusion, Livingstone and Hubel (1984) found that the highest proportions of simple cells occurred in layers 4C α and 4B, which are dominated by magnocellular inputs. Similarly, in our sample 78% of simple cells were localized to the layers with strong magnocellular influence (4C/4C α , 4B, and 6).

From a comparative perspective, the magnocellular influence is interesting because of evidence that the magnocellular pathway is homologous with the pathway arising from the A and A1 layers of the cat lateral geniculate nucleus (Kaplan and Shapley 1982). Considering that experience with the cat visual system led to the original definition of simple and complex

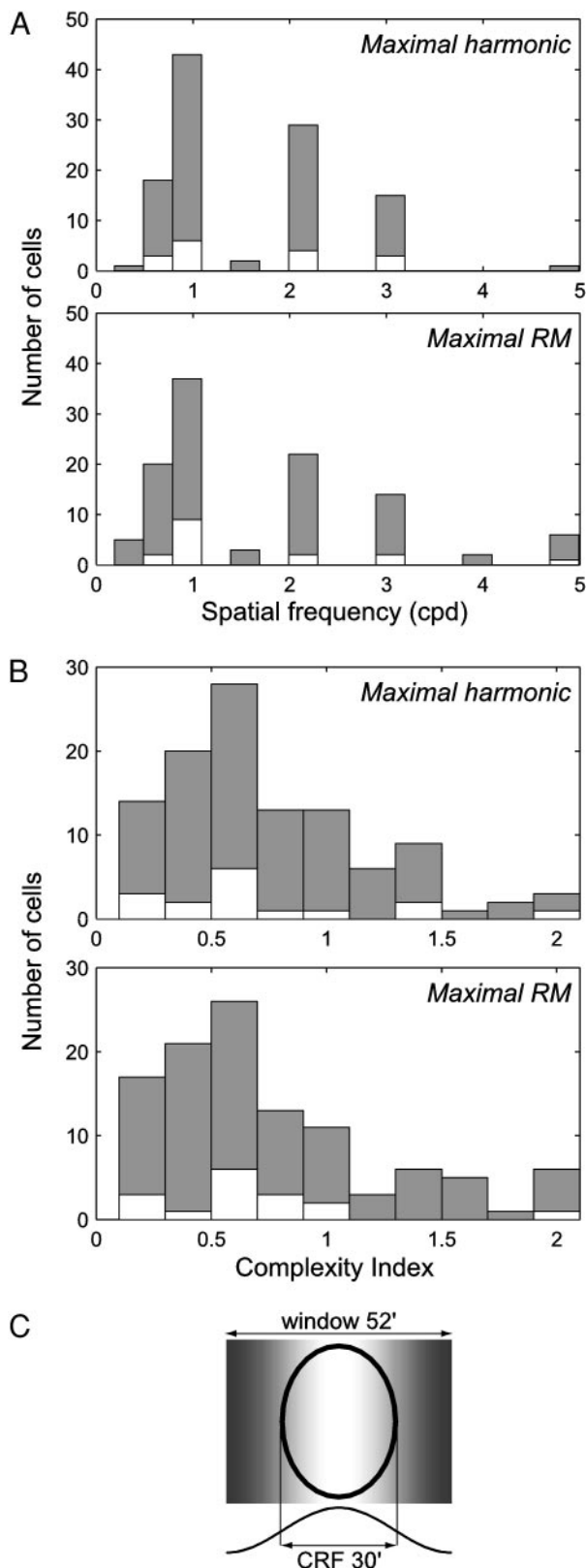


FIG. 10. Spatial frequency and complexity index (CI) distributions. □, simple cells; ■, complex cells. A: spatial frequency distribution. Bin width 0.3 cycles/° (cpd). *Top*: maximal harmonic condition. Mean spatial frequency: 1.53 cpd (simple cells), 1.5 cpd (complex cells). *Bottom*: maximal RM condition. Mean spatial frequency: 1.56 cpd (simple cells), 1.63 cpd (complex cells). B: the distribution of the number of grating cycles that can be fitted within the cell's CRF (CI), calculated as the product of spatial frequency and CRF width. Bin width 0.2 cycle/CRF. *Top*: maximal harmonic condition. *Bottom*: maximal RM condition. For both response criteria, the modes of the CI distributions are around 0.5, implying that the spatial frequency is matched to the size of the CRF. C: relationship among CRF, grating spatial frequency, and window size for 40 complex cells near the mode of CI (0.3 ≤ CI ≤ 0.5). This scaled diagram represents the actual mean values for these parameters for the 40 cells: CRF, 30 minarc; window, 52 minarc; spatial frequency, 1.2 cpd. The luminance profile of the sine wave within the window (1 spatial cycle) is indicated at the *bottom* of the diagram.

cells (Hubel and Wiesel 1962), we are prompted to ask whether there may be a distinct (cat-like) population of “classical” complex cells, as well as a large number of simple cells, in the magnocellular pathway. This line of reasoning suggests that there may be primate complex cells with strong magnocellular dominance (the “classical complex” cells) in addition to other complex cells strongly influenced by the parvocellular pathway, or combinations of magnocellular and parvocellular in-

puts. Such a partitioning might help to explain the great diversity of complex cell responses.

Monocontrast cells

Cells responding to only one sign of contrast have been reported before, but their properties were only qualitatively described (Bullier and Henry 1980) (S1 cells) or different (Schiller et al. 1976) (S1, T cells) from the monocontrast cells of our sample. Our monocontrast cells were characterized by sustained responses to flashes, small ARs, and a low prevalence (4/17 cells) of direction selectivity. They also responded poorly to drifting gratings. Thus these cells seem to be tuned primarily to stationary or slowly moving stimuli of a single sign of contrast. We recently reported that cells activated during the intersaccadic intervals of fixational eye movements, termed *position/drift* cells, included many monocontrast cells (Snodderly et al. 2001). The position/drift cells fire continuously as long as a stationary, steadily illuminated bar is within their CRF but do not respond to the abrupt fixational saccades. In fact, six of eight monocontrast cells tested with a stationary bar were position/drift cells with very small ARs (11 ± 8 minarc). We have suggested that monocontrast cells are probably a separate functional class well suited for coding details of the visual image (Snodderly et al. 2001).

Eye movements and RM

Recently it has been reported that the distribution of RM in alert monkeys is unimodal so that simple and complex cells could not be distinguished (Cumming et al. 1999). Cumming and colleagues attributed this outcome to response phase shifts caused by fixational eye movements. To remove these effects, they analyzed the data in a manner analogous to our “aligned” mode and found a bimodal distribution of RM, with a notch at 0.91 that was suggested to be the basis for a separation. Indeed, if we combined RM distributions of simple and complex cells (e.g., in Fig. 8), we would obtain a distribution with a notch ~ 1 . But the two putative modes of the distribution do not correspond to the classification of cells based on the spatial maps. Our results show that the responses of simple and complex cells are sensitive to fixational eye movements, but taking eye movements into account shifts the RM distributions

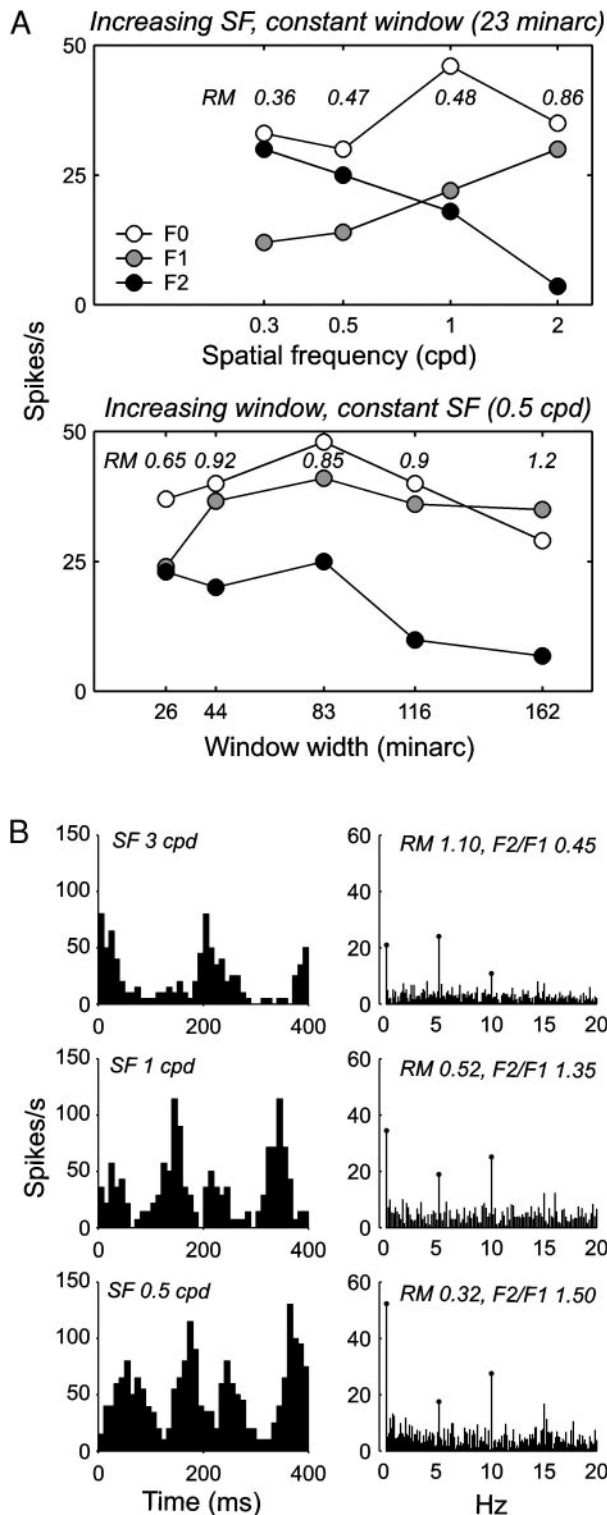


FIG. 11. Effects of spatial frequency and of window width. *A*: interaction between spatial-frequency and window-size effects. *Complex cell 15884* (OI = 0.97; ongoing firing rate 0 spikes/s; CRF, 38 minarc; INCw, 38 minarc; DECw, 30 minarc). *Top*: spatial frequency was changed while the width of the grating window was fixed. The 1st harmonic increased and the 2nd harmonic diminished as spatial frequency increased. *Bottom*: spatial frequency was fixed at 0.5 cpd, and the width of the grating window was increased. Maximal harmonic condition: spatial frequency, 0.5 cpd; window width, 83 minarc. Maximal RM condition: spatial frequency, 0.5 cpd; window width, 162 minarc. *B*: pseudolinear (F1) modulation vs. frequency doubling (F2) in a complex cell. *Left*: PSTH (2 cycles are shown); *right*: harmonic analysis. Spatial frequency (SF) decreases from *top* to *bottom* row. Grating window was 50 minarc, grating temporal frequency, 5 Hz. *Complex cell 18603* (OI, 0.96; ongoing firing rate, 0 spikes/s; CRF, 36 minarc; INCw, 35 minarc; DECw, 36 minarc). Note that as spatial frequency decreases, the RM decreases but the response amplitude (the maximal harmonic, F0 here) increases. Thus in this cell, as in 8 other complex cells, the maximal harmonic condition coincided with the frequency doubling condition (*bottom* row) and hence the low spatial frequency was the most effective one.

toward higher values in *both* simple and complex cells, maintaining considerable overlap between them.

Our conclusion is that simple cells can be identified by a clear separation of INC and DEC ARs in their receptive fields. When phase jitter is removed, simple cells also have $RM > 1$ in response to drifting sinusoidal gratings. However, complex cells have overlapping INC and DEC ARs and a wide range of responses to sinusoidal modulation. Although the complex category includes cells that have unmodulated responses and large receptive fields as expected, it includes many others as well.

Modulation and response diversity of complex cells

When clear F1 modulation is present in the response to a drifting grating but RM is still < 1 , the mean firing rate (F0 harmonic) is usually taken as a measure of the response amplitude. Obviously, when the response is modulated, firing in part of the temporal cycle is low, thus decreasing F0. Therefore when F0 is used as the criterion for choosing the "optimal" stimulus condition, as is commonly done, it biases the conditions toward less modulated responses. In most studies, only the spatial frequency yielding the maximal number of spikes averaged over several stimulus cycles has been tested. However, the spatial frequency eliciting the maximal harmonic is not necessarily the same as the one eliciting the maximal RM as shown in our results (cf. Maloney and Spitzer 1989). Thus the ability of complex cells to produce modulated responses has probably been underestimated. Nevertheless there have been numerous reports of modulated responses of complex cells to drifting gratings (Dean and Tolhurst 1983; Foster et al. 1985; Glezer et al. 1980; Glezer et al. 1982; Hammond et al. 1989; Holub and Morton-Gibson 1981; Kulikowski and Bishop 1982; Pollen and Ronner 1982; Pollen et al. 1978, 1988) as well as evidence of spatial phase-dependent responses (Mechler et al. 1999; Pollen et al. 1988; Spitzer and Hochstein 1985; Victor and Purpura 1998). Furthermore, published distributions of RM show many cells with RM values in the range of 0.5–1 (Dean and Tolhurst 1983; De Valois et al. 1982; O'Keefe et al. 1998; Skottun et al. 1991). In addition, using the *membrane potential modulation index* derived from intracellular recordings in cat V1, Carandini and Ferster (2000) found a continuum of responses, implying that complex cells and simple cells in the mid-range of the continuum should have similarly robust modulation behavior, and Mechler and Ringach (2002) calculated that spike threshold nonlinearity may generate a *bimodal* extracellular RM distribution from the *unimodal* membrane potential modulation index.

Cells with similar RMs may have a quite different harmonic content at frequencies other than F0 and F1. Even an RM as low as 0.5 may belong to a cell with a clearly modulated response that either "rides" on a level of unmodulated firing or spans more than half of a temporal cycle. In these cases, F1 will be significantly elevated above the rest of the spectrum, except for F0. Many cells in our sample behaved in this way in contrast to other cells with comparable values of RM where F1 was no greater than the other spectral components. To understand the diversity within the complex cells, it may be helpful to consider the whole range of spectral components in the neuronal responses.

Some of our stimulus conditions differ from those com-

monly used in studies of anesthetized animals. We note them here so that future comparisons of our data with results from other laboratories can take them into account. Our mean luminance level was relatively low (1 or 5 cd/m^2) because of the need for a relatively large pupil when using the double Purkinje image eyetracker. Otherwise, our general strategy was to choose conditions that were most effective for the cell being studied so that fewer stimuli were required to obtain a good estimate of its response properties. Stimuli were viewed binocularly unless (as occasionally happened) monocular viewing produced a stronger response. We used a monochrome (green or red) grating, because we found one or the other of these stimuli to elicit strong responses from most neurons. Two-thirds of complex cells (60/93), and 12/16 simple cells were tested with green, which had a broad spectrum and was about as effective as white for most cells. The most unusual condition was the use of a red monochrome grating. However, there is no reason to believe it biased our results. The cells tested with green or red showed similar modulation behavior (e.g., mean RM of complex cells was 0.84 ± 0.48 for green and 0.70 ± 0.30 for red).

Implications for modeling

The existing models of complex cells do not account for the effects of varying the stimulus configuration on the response modulation of complex cells. Models based on energy mechanisms that compute the sum of squared outputs of quadrature pairs of linear subunits (Adelson and Bergen 1985; Gaska et al. 1994; Heeger 1991, 1992a,b; Pollen and Ronner 1982, 1983) predict unmodulated responses to drifting gratings, independent of spatial and temporal frequency. It has been proposed that the modulation observed in some complex cells could be explained by incomplete overlap of INC and DEC zones (Heeger 1992b), but the lack of correlation between spatial overlap and modulation speaks against this idea.

Three complex cell models have simulated modulated responses to drifting gratings, but they have two major shortcomings: unrealistic spatial receptive field structures (Maloney and Spitzer 1989) or failure to account for effects of different stimulus configurations (Chance et al. 1999; Garcia-Perez 1999). Thus no existing complex cell model predicts the variety of behaviors exhibited by complex cells. A modeling study based on data gathered with a wide set of stimulus parameters is required to extend the domain of existing models. Because the responses of complex cells to drifting gratings cannot be predicted from responses to bars or counterphase gratings, complex cells clearly violate the superposition principle, and thus their limited pseudolinear behavior is very different from the type of linearity ascribed to simple cells. Simple cells, as a rule, give predictable and robustly modulated responses to all effective gratings, so that only the amplitude but not the form of the response depends on stimulus parameters. Complex cells, on the other hand, frequently show a profound dependence of the response form on the parameters such as spatial frequency and window size. These findings, together with preliminary results obtained with different temporal frequencies, suggest that the time course of interactions between INC and DEC ARs and surrounds may contribute to the diversity of complex cells' responses.

Functional implications

One of the most enduring issues in the physiology of V1 is the function of neurons classified as simple and complex. Simple cells have long been viewed as candidates for edge or feature detection (Hubel and Wiesel 1962), whereas complex cells have been considered to be suited for local Fourier analysis (De Valois et al. 1982; Glezer et al. 1982; Pollen and Ronner 1983). In the framework of the spatial frequency analysis approach, complex cells are thought to represent the amplitude of spatially localized spatial frequency coefficients, invariantly translating small displacements of the stimulus over a restricted region of visual space and performing phase-independent cross-orientation and cross-frequency inhibition tasks (Pollen and Ronner 1983). Our results, as well as results of previous studies (Born and Tootell 1991; Sceniak et al. 2001), suggest that this functional role would be limited to the subset of complex cells with exceptionally large ARs. In monkeys, especially in the alert state, the spatial extent of near optimal gratings is strongly limited by side inhibition, and most cells are tuned to less than two, and frequently less than one, spatial cycle. Many complex cells, especially in the upper and middle layers, have small CRFs, comparable to those of simple cells and thus are able to localize stimuli in space. We suggest that complex cells are well equipped for analyzing spatial position and motion regardless of phase and sign of contrast, whereas simple cells could represent spatial phase information.

The functional significance of modulated responses to drifting gratings remains to be determined. In anesthetized monkeys, drifting gratings evoked the highest information rates in V1 cells with modulated responses and the lowest information rates in unmodulated cells (Reich et al. 2001). However, transient responses to abruptly presented stimuli (Mechler et al. 1998; Muller et al. 2001) may be more applicable to natural vision, where eye movements (Snodderly et al. 2001) and irregularly moving objects create nonperiodic spatiotemporal sequences. This consideration suggests that classical spatial mapping, together with investigation of context effects and response dynamics, may have more utility than steady-state modulation for predicting neuronal contributions to visual function.

It is widely accepted that "linear" simple cells that respond selectively to spatial phase and monotonically to signed contrast are important for understanding the contribution of V1 to visual perception (Wieland et al. 2001). Complex cells have been assigned a secondary role to generalize over space and to perform accessory functions such as normalization and gain control (Carandini et al. 1997; Heeger 1992a; Pollen and Ronner 1983). Although simple cells' properties are useful for at least some aspects of object perception, many functions such as edge detection may benefit from the spatially restricted CRF's of complex cells that generalize over phase and sign of contrast, especially in coping with small displacements during fixation periods. Our results demonstrate that it is important to understand the diversity of complex cells' responses and the influences of their surrounds because complex cells represent the more common functional units in primary visual cortex of primates.

We thank M. Garcia-Perez, D. Pollen, M. Rucci, and two anonymous reviewers for useful comments and C. Simmons for skilled programming assistance.

This work was supported by National Eye Institute Grant EY-12243 and the Fund for the Promotion of Research at the Technion.

REFERENCES

- ADELSON EH AND BERGEN JR. Spatiotemporal energy models for the perception of motion. *J Opt Soc Am A* 2: 284–299, 1985.
- ARTUN OB, SHOUVAL HZ, AND COOPER LN. The effect of dynamic synapses on spatiotemporal receptive fields in visual cortex. *Proc Natl Acad Sci USA* 95: 11999–12003, 1998.
- BORN RT AND TOOTELL RB. Single-unit and 2-deoxyglucose studies of side inhibition in macaque striate cortex. *Proc Natl Acad Sci USA* 88: 7071–7075, 1991.
- BRIDGE H AND CUMMING BG. Responses of macaque v1 neurons to binocular orientation differences. *J Neurosci* 21: 7293–7302, 2001.
- BULLIER J AND HENRY GH. Ordinal position and afferent input of neurons in monkey striate cortex. *J Comp Neurol* 193: 913–935, 1980.
- CARANDINI M AND FERSTER D. Membrane potential and firing rate in cat primary visual cortex. *J Neurosci* 20: 470–484, 2000.
- CARANDINI M AND HEEGER DJ. Summation and division by neurons in primate visual cortex. *Science* 264: 1333–1336, 1994.
- CARANDINI M, HEEGER DJ, AND MOVSHON JA. Linearity and normalization in simple cells of the macaque primary visual cortex. *J Neurosci* 17: 8621–8644, 1997.
- CARANDINI M, MOVSHON JA, AND FERSTER D. Linearity and gain control in V1 simple cells. *Cereb Cortex* 13: 401–443, 1999.
- CHANCE FS, NELSON SB, AND ABBOTT LF. Synaptic depression and the temporal response characteristics of V1 cells. *J Neurosci* 18: 4785–4799, 1998.
- CHANCE FS, NELSON SB, AND ABBOTT LF. Complex cells as cortically amplified simple cells. *Nat Neurosci* 2: 277–282, 1999.
- CONWAY BR. Spatial structure of cone inputs to color cells in alert macaque primary visual cortex (V-1). *J Neurosci* 21: 2768–2783, 2001.
- CUMMING BG AND PARKER AJ. Binocular neurons in V1 of awake monkeys are selective for absolute, not relative, disparity. *J Neurosci* 19: 5602–5618, 1999.
- CUMMING BG, THOMAS OM, PARKER AJ, AND HAWKEN M. J. Classification of simple and complex cells in V1 of the awake monkey. *Soc Neurosci Abstr* 25: 1548, 1999.
- DE VALOIS RL, ALBRECHT DG, AND THORELL LG. Spatial frequency selectivity of cells in macaque visual cortex. *Vision Res* 22: 545–559, 1982.
- DE VALOIS RL, COTTARIS NP, MAHON LE, EL FAR SD, AND WILSON JA. Spatial and temporal receptive fields of geniculate and cortical cells and directional selectivity. *Vision Res* 40: 3685–3702, 2000.
- DEAN AF AND TOLHURST DJ. On the distinctness of simple and complex cells in the visual cortex of the cat. *J Physiol (Lond)* 344: 305–325, 1983.
- DOW BM. Functional classes of cells and their laminar distribution in monkey visual cortex. *J Neurophysiol* 37: 927–946, 1974.
- DOW BM, SNYDER AZ, VAUTIN RG, AND BAUER R. Magnification factor and receptive field size in foveal striate cortex of the monkey. *Exp Brain Res* 44: 213–228, 1981.
- JONES HE, GRIEVE KL, WANG W, AND SILLITO AM. Surround suppression in primate V1. *J Neurophysiol* 86: 2011–2028, 2001.
- ECKHORN R AND THOMAS U. A new method for the insertion of multiple microprobes into neural and muscular tissue, including fiber electrodes, fine wires, needles and microsensors. *J Neurosci Methods* 49: 175–179, 1993.
- FOSTER KH, GASKA JP, NAGLER M, AND POLLEN DA. Spatial and temporal frequency selectivity of neurons in visual cortical areas V1 and V2 of the macaque monkey. *J Physiol (Lond)* 365: 331–363, 1985.
- GARCIA-PEREZ MA. Complex cells as linear mechanisms receiving sequential afferents. *Neuroreport* 10: 3815–3819, 1999.
- GASKA JP, JACOBSON LD, CHEN HW, AND POLLEN DA. Space-time spectra of complex cell filters in the macaque monkey: a comparison of results obtained with pseudowhite noise and grating stimuli. *Vis Neurosci* 11: 805–821, 1994.
- GLEZER VD AND GAUZELMAN VE. Linear and nonlinear properties of simple cells of the striate cortex of the cat: two types of nonlinearity. *Exp Brain Res* 117: 281–291, 1997.
- GLEZER VD, TSHERBACH TA, GAUSELMAN VE, AND BONDARKO VM. Linear and non-linear properties of simple and complex receptive fields in area 17 of the cat visual cortex. A model of the field. *Biol Cybern* 37: 195–208, 1980.

- GLEZER VD, TSHERBACH TA, GAUSELMAN VE, AND BONDARKO VM. Spatio-temporal organization of receptive fields of the cat striate cortex. The receptive fields as the grating filters. *Biol Cybern* 43: 35–49, 1982.
- GUR M, BEYLIN A, AND SNODDERLY DM. Response variability of neurons in primary visual cortex (V1) of alert monkeys. *J Neurosci* 17: 2914–2920, 1997.
- GUR M, BEYLIN A, AND SNODDERLY DM. Physiological properties of macaque V1 neurons are correlated with extracellular spike amplitude, duration, and polarity. *J Neurophysiol* 82: 1451–1464, 1999a.
- GUR M, KAGAN I, AND SNODDERLY DM. “Duplex,” not simple cells are the major cell type in striate cortex of alert monkeys. *Soc Neurosci Abstr* 25: 1548, 1999b.
- GUR M AND SNODDERLY DM. Studying striate cortex neurons in behaving monkeys: benefits of image stabilization. *Vision Res* 27: 2081–2087, 1987.
- GUR M AND SNODDERLY DM. Visual receptive fields of neurons in primary visual cortex (V1) move in space with the eye movements of fixation. *Vision Res* 37: 257–265, 1997a.
- GUR M AND SNODDERLY DM. A dissociation between brain activity and perception: chromatically opponent cortical neurons signal chromatic flicker that is not perceived. *Vision Res* 37: 377–382, 1997b.
- HAMMOND P, POMFRETT CJ, AND AHMED B. Neural motion after-effects in the cat’s striate cortex: orientation selectivity. *Vision Res* 29: 1671–1683, 1989.
- HEEGER DJ. Nonlinear model of neural responses in cat visual cortex. In: *Computational Models of Visual Processing*, edited by Landy MS and Movshon JA. Cambridge: The MIT Press, 1991, p. 119–133.
- HEEGER DJ. Normalization of cell responses in cat striate cortex. *Vis Neurosci* 9: 181–197, 1992a.
- HEEGER DJ. Half-squaring in responses of cat striate cells. *Vis Neurosci* 9: 427–443, 1992b.
- HEEGER DJ. Modeling simple-cell direction selectivity with normalized, half-squared, linear operators. *J Neurophysiol* 70: 1885–1898, 1993.
- HEEGER DJ, SIMONCELLI EP, AND MOVSHON JA. Computational models of cortical visual processing. *Proc Natl Acad Sci USA* 93: 623–627, 1996.
- HEGGELUND P. Quantitative studies of the discharge fields of single cells in cat striate cortex. *J Physiol (Lond)* 373: 277–292, 1986.
- HOLUB RA AND MORTON-GIBSON M. Response of visual cortical neurons of the cat to moving sinusoidal gratings: response-contrast functions and spatio-temporal interactions. *J Neurophysiol* 46: 1244–1259, 1981.
- HUBEL DH AND WIESEL TN. Receptive fields, binocular interactions and functional architecture in the cat’s visual cortex. *J Physiol (Lond)* 160: 106–154, 1962.
- HUBEL DH AND WIESEL TN. Receptive fields and functional architecture of monkey striate cortex. *J Physiol (Lond)* 195: 215–243, 1968.
- KAPLAN E AND SHAPLEY RM. X and Y cells in the lateral geniculate nucleus of macaque monkeys. *J Physiol (Lond)* 330: 125–143, 1982.
- KULIKOWSKI JJ AND BISHOP PO. Silent periodic cells in the cat striate cortex. *Vision Res* 22: 191–200, 1982.
- LI W, THEIR P, AND WEHRHAHN C. Contextual influence on orientation discrimination of humans and responses of neurons in V1 of alert monkeys. *J Neurophysiol* 83: 941–954, 2000.
- LIVINGSTONE MS. Mechanisms of direction selectivity in macaque V1. *Neuron* 20: 509–526, 1998.
- LIVINGSTONE MS AND HUBEL DH. Anatomy and physiology of a color system in the primate visual cortex. *J Neurosci* 4: 309–356, 1984.
- MALONEK D AND SPITZER H. Response histogram shapes and tuning curves: the predicted responses of several cortical cell types to drifting gratings stimuli. *Biol Cybern* 60: 469–475, 1989.
- MAZER JA, VINJE WE, MCDERMOTT J, SCHILLER PH, AND GALLANT JL. Spatial frequency and orientation tuning dynamics in area V1. *Proc Natl Acad Sci USA* 99: 1645–1650, 2002.
- MECHLER F, VICTOR JD, PURPURA KP, AND SHAPLEY R. Robust temporal coding of contrast by V1 neurons for transient but not for steady-state stimuli. *J Neurosci* 18: 6583–6598, 1998.
- MECHLER F, REICH DS, AND VICTOR JD. In V1 complex cells, phase-sensitive receptive field nonlinearities signal a variety of spatial features and violate a pure energy-operator model. *Soc Neurosci Abstr* 25: 1932, 1999.
- MECHLER F AND RINGACH DL. On the classification of simple and complex cells. *Vision Res* 42: 1017–1033, 2002.
- MOVSHON JA, THOMPSON ID, AND TOLHURST DJ. Receptive field organization of complex cells in the cat’s striate cortex. *J Physiol (Lond)* 283: 79–99, 1978.
- MULLER JR, METHA AB, KRAUSKOPF J, AND LENNIE P. Information conveyed by onset transients in responses of striate cortical neurons. *J Neurosci* 21: 6978–6990, 2001.
- O’KEEFE LP, LEVITT JB, KIPER DC, SHAPLEY RM, AND MOVSHON JA. Functional organization of owl monkey lateral geniculate nucleus and visual cortex. *J Neurophysiol* 80: 594–609, 1998.
- PETERHANS E, BISHOP PO, AND CAMARDA RM. Direction selectivity of simple cells in cat striate cortex to moving light bars. I. Relation to stationary flashing bar and moving edge responses. *Exp Brain Res* 57: 512–522, 1985.
- PETTIGREW JD, NIKARA T, AND BISHOP PO. Responses to moving slits by single units in cat striate cortex. *Exp Brain Res* 6: 373–390, 1968.
- POLLEN DA, ANDREWS BW, AND FELDON SE. Spatial frequency selectivity of periodic complex cells in the visual cortex of the cat. *Vision Res* 18: 665–682, 1978.
- POLLEN DA, GASKA JP, AND JACOBSON LD. Responses of simple and complex cells to compound sine-wave gratings. *Vision Res* 28: 25–39, 1988.
- POLLEN DA AND RONNER SF. Spatial computation performed by simple and complex cells in the visual cortex of the cat. *Vision Res* 22: 101–118, 1982.
- POLLEN DA AND RONNER SF. Visual cortical neurons as localized spatial frequency filters. *IEEE Trans System, Man Cybern* 13: 907–916, 1983.
- PRINCE SJ, POINTON AD, CUMMING BG, AND PARKER AJ. The precision of single neuron responses in cortical area V1 during stereoscopic depth judgments. *J Neurosci* 20: 3387–3400, 2000.
- REICH DS, MECHLER F, AND VICTOR JD. Formal and attribute-specific information in primary visual cortex. *J Neurophysiol* 85: 305–318, 2001.
- ROSSI AF, DESIMONE R, AND UNGERLEIDER LG. Contextual modulation in primary visual cortex of macaques. *J Neurosci* 21: 1698–1709, 2001.
- SCENIAK MP, HAWKEN MJ, AND SHAPLEY R. Visual spatial characterization of macaque V1 neurons. *J Neurophysiol* 85: 1873–1887, 2001.
- SCENIAK MP, RINGACH DL, HAWKEN MJ, AND SHAPLEY R. Contrast’s effect on spatial summation by macaque V1 neurons. *Nat Neurosci* 2: 733–739, 1999.
- SCHILLER PH, FINLAY BL, AND VOLMAN SF. Quantitative studies of single-cell properties in monkey striate cortex. I. Spatiotemporal organization of receptive fields. *J Neurophysiol* 39: 1288–1319, 1976.
- SKOTTUN BC, DE VALOIS RL, GROSOF DH, MOVSHON JA, ALBRECHT DG, AND BONDS AB. Classifying simple and complex cells on the basis of response modulation. *Vision Res* 31: 1079–1086, 1991.
- SNODDERLY DM. Extracellular single unit recording. In: *Bioelectric Recording Techniques. Cellular Processes and Brain Potentials*, edited by Thompson RF and Patterson MM. New York: Academic, 1973, p. 137–163.
- SNODDERLY DM. Effects of light and dark environments on macaque and human fixational eye movements. *Vision Res* 27: 401–415, 1987.
- SNODDERLY DM AND GUR M. Organization of striate cortex of alert, trained monkeys (*Macaca fascicularis*): ongoing activity, stimulus selectivity, and widths of receptive field activating regions. *J Neurophysiol* 74: 2100–2125, 1995.
- SNODDERLY DM, KAGAN I, AND GUR M. Simple cells and other cells in striate cortex of alert monkeys (Abstract). *Invest Ophthalmol Vis Sci* 41: S53, 2000.
- SNODDERLY DM, KAGAN I, AND GUR M. Selective activation of visual cortex neurons by fixational eye movements: implications for neural coding. *Vis Neurosci* 18: 259–277, 2001.
- SNODDERLY DM AND KURTZ D. Eye position during fixation tasks: comparison of macaque and human. *Vision Res* 25: 83–98, 1985.
- SPITZER H AND HOCHSTEIN S. Simple- and complex-cell response dependences on stimulation parameters. *J Neurophysiol* 53: 1244–1265, 1985.
- TROYER TW, KRUKOWSKI AE, PRIEBE NJ, AND MILLER KD. Contrast-invariant orientation tuning in cat visual cortex: thalamocortical input tuning and correlation-based intracortical connectivity. *J Neurosci* 18: 5908–5927, 1998.
- VICTOR JD AND PURPURA KP. Spatial phase and the temporal structure of the response to gratings in V1. *J Neurophysiol* 80: 554–571, 1998.
- VINJE WE AND GALLANT JL. Natural stimulation of the nonclassical receptive field increases information transmission efficiency in V1. *J Neurosci* 22: 2904–2915, 2002.
- VON DER HEYDT R, PETERHANS E, AND DURSTELER MR. Periodic-pattern-selective cells in monkey visual cortex. *J Neurosci* 12: 1416–1434, 1992.
- WIELAARD DJ, SHELLEY M, MCLAUGHLIN D, AND SHAPLEY R. How simple cells are made in a nonlinear network model of the visual cortex. *J Neurosci* 21: 5203–5211, 2001.
- ZHOU H, FRIEDMAN HS, AND VON DER HEYDT R. Coding of border ownership in monkey visual cortex. *J Neurosci* 20: 6594–6611, 2000.